



**HAL**  
open science

# Exploring the landscape and climatic conditions of Neanderthals and anatomically modern humans in the Middle East: the rodent assemblage from the late Pleistocene of Kaldar Cave (Khorramabad Valley, Iran)

Ivan Rey-Rodríguez, Juan Manuel Lopez-García, Blain Hugues-Alexandre, Emmanuelle Stoetzel, Christiane Denys, Mónica Fernández-García, Laxmi Tumung, Behrouz Bazgir

## ► To cite this version:

Ivan Rey-Rodríguez, Juan Manuel Lopez-García, Blain Hugues-Alexandre, Emmanuelle Stoetzel, Christiane Denys, et al.. Exploring the landscape and climatic conditions of Neanderthals and anatomically modern humans in the Middle East: the rodent assemblage from the late Pleistocene of Kaldar Cave (Khorramabad Valley, Iran). *Quaternary Science Reviews*, 2020, 236, pp.106278. 10.1016/j.quascirev.2020.106278 . hal-02568534

**HAL Id: hal-02568534**

**<https://hal.science/hal-02568534>**

Submitted on 10 Nov 2020

**HAL** is a multi-disciplinary open access archive for the deposit and dissemination of scientific research documents, whether they are published or not. The documents may come from teaching and research institutions in France or abroad, or from public or private research centers.

L'archive ouverte pluridisciplinaire **HAL**, est destinée au dépôt et à la diffusion de documents scientifiques de niveau recherche, publiés ou non, émanant des établissements d'enseignement et de recherche français ou étrangers, des laboratoires publics ou privés.



Distributed under a Creative Commons Attribution - NonCommercial - NoDerivatives 4.0 International License

1 **Exploring the landscape and climatic conditions of Neanderthals and**  
2 **anatomically modern humans in the Middle East: the rodent assemblage**  
3 **from the late Pleistocene of Kaldar Cave (Khorramabad Valley, Iran)**

4  
5 Iván Rey-Rodríguez <sup>a,b \*</sup>, Juan-Manuel López-García <sup>c,d</sup>, Hugues-Alexandre  
6 Blain <sup>c,d</sup>, Emmanuelle Stoetzel <sup>a</sup>, Christiane Denys <sup>e</sup>, Mónica Fernández-García  
7 <sup>b,a</sup>, Laxmi Tumung <sup>c,d,a</sup>, Andreu Ollé <sup>c,d</sup>, Behrouz Bazgir <sup>d</sup>

8  
9 <sup>a</sup> HNHP UMR 7194, CNRS / Muséum national d'Histoire naturelle / UPVD / Sorbonne  
10 Universités, Musée de l'Homme, Palais de Chaillot, 17 place du Trocadéro, 75016 Paris, France

11 <sup>b</sup> Sezione di Scienze Preistoriche e Antropologiche, Dipartimento di Studi Umanistici, Università  
12 degli Studi di Ferrara, C.so Ercole I d'Este, 32 - 44121 Ferrara, Italy

13 <sup>c</sup> Institut Català de Paleoecologia Humana i Evolució Social (IPHES). Zona Educacional 4,  
14 Campus Sescelades URV (Edifici W3) 43007 Tarragona, Spain

15 <sup>d</sup> Àrea de Prehistòria, Universitat Rovira i Virgili. Facultat de Lletres, Avinguda Catalunya 35,  
16 43002 Tarragona, Spain

17 <sup>e</sup> ISYEB UMR 7205, CNRS / Muséum national d'Histoire naturelle / UPMC / EPHE / Sorbonne  
18 Universités, Paris, France

19 \* **corresponding author:** ivan.rey-rodriguez@edu.mnhn.fr / ivanreyrguez@gmail.com (Iván  
20 Rey-Rodríguez)

21  
22 **Abstract**

23 The Middle East, specially the Zagros region, lies in a strategic position as a  
24 crossroads between Africa, Europe and eastern Asia. The landscape of this  
25 region that prevailed around the Neanderthal and anatomically modern human  
26 occupations is not well known. Only a few sites have been studied in detail in  
27 this area, often providing only a faunal list. These reveal that Neanderthals and  
28 anatomically modern humans lived in a landscape mainly composed of dry  
29 steppes.

30 Here we extend the data obtained from Kaldar Cave through a systematic  
31 study of the rodent assemblage. The site provided evidence of a Pleistocene  
32 occupation attested by lithic tools associated with the Middle and Upper  
33 Palaeolithic, but it was also occupied during the Holocene, as evidenced by  
34 Neolithic artefacts. First excavations have revealed small vertebrates in Layer 4  
35 (sub-layer 5 and 5II), belonging to the Upper Palaeolithic, and Layer 5 (sub-  
36 layers 7 and 7II), belonging to the Middle Palaeolithic.

37 The rodent assemblage of Kaldar Cave is mainly composed of six arvicoline,  
38 two cricetine, one glirid, one dipodid, one gerbilline and two murine species.

39 This assemblage shows that during the Late Pleistocene the environment  
40 around the site was mainly composed of open dry steppes, as indicated by the  
41 most abundant taxa, *Microtus*, *Ellobius* and *Meriones*. However, murine species  
42 indicate the presence of a vegetation cover. The palaeoclimatic conditions are  
43 characterised by lower temperatures and also less precipitation than at present.

44 The results obtained with the rodent assemblages show that there is no  
45 major palaeoenvironmental or palaeoclimatic change that would explain the

46 cultural shift between Layer 5 (Middle Palaeolithic) and Layer 4 (Upper  
47 Palaeolithic).

48

49 **Keywords:** *Rodentia, Middle East, taxonomy, palaeoecology, human*  
50 *occupations*

51

52

## 53 1. Introduction

54

55 Small vertebrates are recognized to be good palaeoecological indicators due  
56 to their rapid evolution, the limited geographic range of a species and unique  
57 niche requirements, as well as their frequent preservation in archaeological and  
58 palaeontological sites. They might be excellent indicators of palaeovegetation  
59 type and provide a high-resolution proxy for palaeoenvironmental changes (e.g.  
60 Belmaker and Hovers, 2011). Studies of small vertebrates from archaeological  
61 sites in the Middle East are still scarce (Belmaker and Hovers, 2011; Belmaker  
62 et al., 2016; Demirel et al., 2011; Fernández-Jalvo, 2016a; Kandel et al., 2017;  
63 Maul et al., 2015a, 2015b; Smith et al., 2015; Weissbrod and Zaidner, 2014),  
64 and they mainly propose preliminary lists of taxa. On the other hand, some  
65 studies of extant owl pellet assemblages have been performed in the Middle  
66 East (Abi-said et al., 2014; Darvish et al., 2000; Haddadian Shad et al., 2014;  
67 Kopij and Liven-schulman, 2013; Obuch and Khaleghizadeh, 2012; Rey-  
68 Rodríguez et al., 2019; Shehab et al., 2013), providing taxonomic and some  
69 taphonomic reference data in Iran, Lebanon, Israel, Turkey and Syria.

70 The main palaeoecological and palaeoclimatic reconstructions based on  
71 faunal assemblages relate to the unique niche requirements of a particular  
72 species. Belmaker *et al.* (2011) pointed out that their interpretations, in contrast,  
73 are based on analyses of community composition. Analyses of persistence  
74 *versus* change over time should take into account species presence-absence,  
75 rank abundance and proportional abundance (Belmaker and Hovers, 2011).

76 The Middle East is a prime location to study Neanderthal and anatomically  
77 modern human (AMH) interactions during the Middle to Upper Palaeolithic  
78 transition (Belmaker et al., 2016). However, sites yielding evidence of both  
79 Neanderthal and AMH occupations in the same sequence are rare, only five  
80 sites were well excavated (Bazgir et al., 2014; Bazgir et al., 2017). In this  
81 framework, Kaldar Cave is a key archaeological site for evaluating the influence  
82 of environment on cultural changes in both human species because of its  
83 location and the faunal and lithic remains. The main objective of this paper is to  
84 infer the landscape composition and the climatic conditions in which  
85 Neanderthal and AMH populations pursued their activities through the study of  
86 small mammals. We identify and describe the rodent fossils recovered from  
87 Kaldar Cave in order to establish the main criteria for further identifications in  
88 this region and provide a preliminary basis for future systematic studies.

89

90

## 91 **2. Kaldar Cave**

92

93 Kaldar Cave is located in the northern part of the Khorramabad valley,  
94 Lorestan Province, western Iran (48°17'35" E, 33°33'25" N) at 1290 m a.s.l.  
95 (Fig. 1a,b). The cave was discovered in 2007, and the first archaeological  
96 intervention was undertaken by an Iranian-Spanish team in 2011-2012,  
97 revealing the great potential of the cave (Bazgir et al., 2014). A second  
98 excavation was performed in 2014-2015. The trench exposed an approximately  
99 2m-thick section of sedimentary deposits, characterized by 5 main layers,  
100 themselves divided into several sub-layers (Fig. 1c).

101 Layer 5 (including sub-layers 7 and 7II) consists of an extremely cemented  
102 reddish-brown sediment with some small angular limestone blocks and Middle  
103 Palaeolithic artefacts with Levallois elements. So far, no chronometric data are  
104 available for this layer (Bazgir et al., 2017).

105 Layer 4 (including sub-layers 5, 5II, 6 and 6II) consists of a silty but compact  
106 dark-brown sediment with cultural remains attributed to the Upper and early  
107 Upper Palaeolithic. In the uppermost parts of this layer, two fireplaces made of  
108 clay were recovered and dated through thermoluminescence, yielding ages that  
109 ranged from 23,100 ± 3 300 to 29,400 ± 2 300 BP (Bazgir et al., 2017). The  
110 dates obtained show that these fireplaces were made or re-used from existing  
111 older sediment from the upper part of this layer in the later stages of the Upper  
112 Palaeolithic. AMS radiocarbon dates of 38,650–36,750 cal BP, 44,200–42,350  
113 cal BP, and 54,400–46,050 cal BP have been obtained from charcoal material  
114 located below this layer (Bazgir et al., 2017; Becerra-Valdivia et al., 2017).

115 Layers 1 to 3 (including sub-layers 4 and 4II) consist of ashy sediments of a  
116 blackish-green colour containing both thick and thin angular limestone clasts.  
117 These layers varied in thickness from 60 to 90 cm and contained many phases  
118 dating to the Holocene: Islamic and historical eras, Iron Age, Bronze Age,  
119 Chalcolithic and Neolithic. However, due to the presence in these layers of  
120 bioturbation mainly by burrowing animals, the phases were recognized only by  
121 a preliminary study of the potsherds, metal artefacts and some diagnostic lithic  
122 artefacts from the lower layers.

123 This site provides evidence for the Middle to Upper Palaeolithic transition in  
124 the Middle East (Bazgir et al., 2017). Moreover, Kaldar Cave has yielded the  
125 oldest evidence of *Prunus* spp. in the area, through the study of thirty charcoal  
126 remains (Allué et al., 2018), that helps us to reconstruct the environmental  
127 conditions, evidencing a wooded vegetation.

128

## 129 **3. Material and methods**

130

131 The rodent fossil remains used in this study, 1112 molars, come from the  
132 archaeological excavation campaigns carried out in Kaldar Cave in 2011-2012  
133 and 2014-2015.

134 The samples comprise disarticulated bones and isolated teeth that were  
135 collected in the field by water screening using superimposed 5 and 0.5 -mm  
136 mesh screens.

137

### 138 **3.1. Taxonomy**

139

140 In this article we only focus on rodents, because these are one of the most  
141 useful tools for palaeoenvironmental and palaeoclimatic reconstructions of  
142 archaeological sites, and the other material, as amphibians, squamates, birds,  
143 shrews and bats, will be studied later. The taxonomic identification of the rodent  
144 remains is based mainly on molar morphology and measurements of the lower  
145 m1, the taxonomically most diagnostic tooth.

146 The remains were identified at a specific level whenever possible, thanks to  
147 comparisons with reference collections from the Natural History Museum of  
148 London (NHM) and comparative morphological and biometric data from the  
149 literature, notably for *Microtus* (Coşkun, 2016; Kryštufek and Shenbrot, 2016;  
150 Kryštufek and Vohralík, 2009; López-García, 2011; Rusin, 2017; Shenbrot,  
151 Kryštufek et al. 2016; Tesakov, 2016), *Cricetulus* (Bogicevic et al., 2011;  
152 Kryštufek et al., 2017; Sándor, 2018), *Mesocricetus* (Kryštufek and Vohralík,  
153 2009), *Meriones* (Coşkun, 1999; Darvish, 2011; Dianat et al., 2017; Kryštufek  
154 and Vohralík, 2009; Souttou and Denys, 2012; Stoetzel et al., 2017), *Allactaga*  
155 (Karami et al., 2008; Shenbrot, 2009), *Myomimus* (Gerrie and Kennerley, 2017;  
156 Karami et al., 2008; Kennerley and Kryštufek, 2019), *Apodemus* (Amori et al.,  
157 2016; Bogicevic et al., 2011; Knitlová and Horáček, 2017; Kryštufek and  
158 Vohralík, 2009; López-García, 2008) and *Mus* (Darviche et al., 2006; Kryštufek  
159 and Vohralík, 2009; Siahsarvie and Darvish, 2008).

160 Quantification of taxonomic frequencies was based on standard measures in  
161 zooarchaeological analyses, including the number of identified specimens  
162 (NISP) and minimum number of individuals (MNI) (Weissbrod and Zaidner,  
163 2014). This latter was estimated using the most abundant skeletal element  
164 present in the assemblage (molars in our case).

165

### 166 **3.2. Taphonomic remarks**

167

168 A preliminary study was performed on the Kaldar Cave micromammal  
169 remains. This was based on the systematic descriptive method that examines  
170 the modifications of prey bones induced by predation, focusing on the degree of  
171 digestion observed in teeth during the identification (Andrews, 1990;  
172 Fernández-Jalvo et al., 2016). This study showed a significant number of  
173 digested teeth (Bazgir et al., 2017), indicating that predation activity was the  
174 origin of at least part of the accumulation. According to the different degrees of  
175 digestion (mostly light, moderate and, heavy in a few cases) observed in the  
176 molars, the predator responsible for this accumulation could be a category 3  
177 predator such as the tawny owl (*Strix aluco*) or the Eurasian eagle owl (*Bubo*

178 *bubo*). Both species are currently present in the area, have opportunistic  
179 hunting habits, and are sedentary, so their prey spectrum is assumed to be a  
180 good representation of the ecosystem in which they live.

181

### 182 **3.3. Palaeoenvironmental and palaeoclimatic reconstructions**

183

#### 184 *3.3.1. Habitat weighting method*

185

186 Palaeoecological interpretations derived from faunal data are based on  
187 analyses of community composition (Belmaker and Hovers, 2011). The method  
188 used for the palaeoenvironmental reconstruction is the *habitat weighting*  
189 *method*, also named the *taxonomic habitat index* (Evans et al., 1981; Andrews,  
190 2006; modified by Blain et al., 2008; López-García et al., 2011), which is based  
191 on the current distribution of each taxon in the habitat(s) where it can be found  
192 nowadays. We assume that the Kaldar Cave species had equivalent ecological  
193 requirements to their present-day relatives, because the Late Pleistocene  
194 species are the same as those today and no extinct fossil species are found in  
195 the assemblage. We adapt the method to our studied area, differentiating the  
196 following types of habitats: Forest (Fo), a large area covered with trees;  
197 Shrubland (Sh), vegetation dominated by shrubs; Grassland (Gr), an open area  
198 covered with grass; Desert (De), an area with little precipitation and no  
199 vegetation cover; Wetland (We), an area where water covers the soil; Steppe  
200 (St), a dry grassy plain; and Rocky (Ro), a rocky or stony substrate. Each  
201 species has a score of 1.00, which is divided between the habitats where the  
202 species can be found at present (Table 1), all the species ranges were taken  
203 from the IUCN Red List of Threatened Species  
204 (<https://www.iucnredlist.org/resources/spatial-data-download>).

205

#### 206 *3.3.2. Bioclimatic Model*

207

208 In order to reconstruct the climate at Kaldar Cave, we applied the *bioclimatic*  
209 *model (BM)*, which was developed by Hernández-Fernández (2001) on the  
210 basis of the faunal spectrum, assuming that small- and large-mammal species  
211 can be ascribed to ten different climates (Hernández-Fernández, 2001;  
212 Hernández-Fernández and Peláez-Campomanes, 2003; Hernández-Fernández  
213 et al., 2007). It was first necessary to calculate the climatic restriction index  
214 ( $CRI_i = 1/n$ , where  $i$  is the climatic zone where the species appear and  $n$  is the  
215 number of zones where the species is present) and the bioclimatic component  
216 ( $BC_i = (\sum CRI_i) 100/S$ , where  $i$  is the climatic zone and  $S$  is the number of  
217 species). To BC a mathematical model is applied as a regression that allows us  
218 to calculate climatic parameters (see Appendix 1).

219

220 The different climatic groups defined by Hernández-Fernández (2001) and  
221 Hernández-Fernández et al. (2007) are: I *equatorial*; II *tropical with summer*  
*rains*; II/III *transition tropical semiarid*; III *sub-tropical arid*; IV, *subtropical with*

222 winter rains and summer droughts; V, *warm temperate* with not very severe  
223 winters but high humidity; VI, *typical temperate* with winters that are cold but not  
224 very long, but summers that are cool; VII, *arid-temperate* with large temperature  
225 contrasts between winter and summer; VIII, *cold-temperate* with cool summers  
226 and long cold winters (boreal) and IX, *artic* (Table 2).

227 By means of the *BM* we were able to estimate the mean annual temperature  
228 (MAT), the mean temperature of the coldest month (MTC), the mean  
229 temperature of the warmest month (MTW) and the mean annual precipitation  
230 (MAP). This method also allowed us to assess whether there were changes in  
231 the temperature and precipitation regimes during the Middle to Upper  
232 Palaeolithic transition at Kaldar Cave.

233

## 234 **4. Results and discussion**

235

### 236 **4.1. Taxonomic identifications**

237

238 In total 264 minimum number of individuals (MNI) were identified (Table 3  
239 and Fig. 2). Some differences were found with respect to the preliminary list  
240 previously published by Bazgir et al. (2017). We notably found some new  
241 specimens and reconsidered the identifications for *Ellobius talpinus*,  
242 *Calomyscus* sp. and *Dryomys* cf. *nitedula*.

243

#### 244 **Order Rodentia Bowdich, 1821**

245

##### **Rodentia indet.**

246

247 There are 14 teeth (11 in Layer 4 and 3 in Layer 5) that have not been identified  
248 to the family or genus level because they were broken.

249

#### 250 **Family Cricetidae Fisher, 1817**

251

##### **Subfamily Arvicolinae Gray, 1821**

252

##### **Genus *Microtus* Schrank, 1798**

253

##### ***Microtus* spp.**

254

255 **Material:** 554 isolated teeth. **Layer 1-3:** four isolated teeth; three left lower  
256 m1 and one right lower m1. **Layer 4:** 258 isolated teeth; 81 m2; 101 m3, 13  
257 right upper M1, 31 right lower m1; four left upper M1 and 28 left lower m1.  
258 **Layer 5:** 292 isolated teeth; 119 m2; 53 m3; nine left upper M1, 51 left lower  
259 m1; 10 right upper M1; 50 right lower m1.

260

#### 261 ***Microtus socialis* Pallas, 1773**

262

263 **Material:** 74 isolated teeth. **Layer 1-3:** three isolated teeth, three right lower  
264 m1. **Layer 4:** 36 isolated teeth; 20 right lower m1 and 16 left lower m1. **Layer 5:**  
265 35 isolated teeth; 20 right lower m1 and 15 left lower m1.

266

267

**Microtus irani Thomas, 1921**

268

269 **Material:** 15 isolated teeth. **Layer 1-3:** one isolated tooth, one right lower m1.

270

**Layer 5:** 14 isolated teeth; nine right lower m1 and five left lower m1.

271

272

**Microtus guentheri Danford & Alston, 1880**

273

274 **Material:** 17 isolated teeth. **Layer 1-3:** one isolated tooth, one left lower m1.

275

**Layer 4:** 16 isolated teeth; nine right lower m1 and seven left lower m1.

276

277

**Description and discussion:** all the molars are hypsodont and arhizodont with crown cementum in the re-entrant angles. The enamel differentiation is *Microtus*-like. Six extant species of *Microtus* have been identified in Iran: *Microtus arvalis*, *Microtus irani*, *Microtus kermanensis*, *Microtus socialis*, *Microtus transcaspicus* and *Microtus guentheri* (Aşan Baydemir and Duman, 2009; Golenishchev et al., 2019; Firouz, 2005).

282

283

*Microtus* m1 are characterized by four buccal and five lingual re-entrant angles (Kryštufek and Vohralík, 2009; Tsytsulina et al., 2017) with a posterior lobe (PL), seven triangles (T) and an anterior cap (AC). We identified the Kaldar specimens on the basis of their measurements (Table 4), the arrangement and morphology of the triangles, and the AC (which may or may not be connected with the other elements).

288

In our sample we identified *Microtus* spp., *Microtus socialis*, *Microtus guentheri* and *Microtus irani*.

290

291

In *Microtus socialis*, the triangles from T1-T5 are closed, but T6-T7 are parallel and broadly confluent with the AC. *Microtus guentheri* is distinguishable from *Microtus socialis* by the rounded shape of the AC, which is of an arhombomorph type (Aşan Baydemir and Duman, 2009), and also by T6-T7, which are separated from the AC. In accordance with the measurements given in Aşan Baydemir et al. (2009), the size of *Microtus guentheri* and *Microtus socialis* is similar. In *Microtus irani*, triangles T1-T5 are closed, but T6-T7 are open and not parallel with one another; moreover, *Microtus irani* is clearly larger than the other species considered in our reference collection and also in our sample. Finally, we include in *Microtus* spp. all the elements that we cannot attribute to one species or another, in particular because of their bad state of preservation (due to digestion, breakage).

302

**Habitat and distribution:** *Microtus irani* occupies grasslands in Iran, Turkey and the Caucasus (Kryštufek and Kefelioğlu, 2001).

304

305

*Microtus socialis* is found in Russia, Ukraine, the Caucasus, Transcaucasia, Turkestan, Iran and Afghanistan (Tsytsulina et al., 2017), although the range is fragmented. It is a highly colonial species, found in steppe habitats and also in agricultural lands, but extending also to bushy scrubs and uncultivated mountain valleys, as well as to open oak forests on dry hillsides (Tsytsulina et al., 2017).

309



310 *Microtus guentheri* occurs from the southeastern Balkans and Turkey through  
311 Syria, Lebanon and Israel, with an isolated range segment in northern Libya,  
312 Iran and some parts of Europe (Aşan Baydemir and Duman, 2009). This  
313 species is present in dry grasslands with sparse vegetation (Amr, 2015).

314

315

**Genus *Chionomys* Miller, 1908**

316

***Chionomys nivalis* Martins, 1842**

317

318 **Material:** 25 isolated teeth. **Layer 1-3:** two isolated teeth; one left lower m1  
319 and one right lower m1. **Layer 4:** 17 isolated teeth; 12 right lower m1; five left  
320 lower m1. **Layer 5:** six isolated teeth; three left lower m1; three right lower m1.

321

322 **Description and discussion:** in our specimens it can be observed that the  
323 first lower molars display five triangles and that the morphology of the  
324 anteroconid complex (AC) is characteristic of the *nivalis* morphotype, where  
325 triangles T6 and T7 are absent and the anterior cap is of an arrowhead or oval  
326 shape, inclined towards the labial part. The enamel is of the *Microtus* type with  
327 cement (Krystufek, 2017; Kryštufek and Vohralík, 2009; López-García, 2011).  
328 These specimens differ from *Microtus* in that they only have five triangles, and  
329 the morphology of the AC is the other main characteristic of this species that  
330 helps us to differentiate it from *Microtus*.

330

331 **Habitat and distribution:** *Chionomys nivalis* has a global distribution  
332 extending from southwestern Europe through southeastern Europe to the  
333 Caucasus, Turkey, Israel, Lebanon, Syria and Iran. In Iran it is distributed in the  
334 north and also in the west (Shenbrot and Krasnov, 2005; Krystufek, 2017). This  
335 is the only *Chionomys* species occurring today in Iran, but two other species (*C.*  
336 *gud*, *C. roberti*) are represented a little further north (northeastern Turkey,  
337 southern Georgia).

338 Regarding its habitat, it is present in open rocky areas, typically above the tree  
339 line and with scarce vegetation cover (Amori, 1999).

339

340

**Genus *Ellobius* Fischer, 1814**

341

***Ellobius* spp.**

342

343 **Material:** 173 isolated teeth. **Layer 1-3:** two isolated teeth; two left lower m1.  
344 **Layer 4:** 91 isolated teeth; seven indet.; eight right lower m1; five left lower m1;  
345 11 upper M1; 43 m2; 17 m3. **Layer 5:** 80 isolated teeth; seven left lower m1;  
346 three upper M1; 45 m2; 25 m3.

347

348

***Ellobius fuscocapillus* Blyth, 1843**

349

350 **Material:** 11 isolated teeth. **Layer 1-3:** one isolated tooth; one right lower m1.  
351 **Layer 4:** five isolated teeth; two right lower m1; three left lower m1. **Layer 5:**  
352 five isolated teeth; four left lower m1 and one right lower m1.

353

### *Ellobius lutescens* Thomas, 1897

354  
355

356 **Material:** 20 isolated teeth. **Layer 4:** 10 isolated teeth; seven right lower m1  
357 and three left lower m1. **Layer 5:** 10 isolated teeth; four left lower m1 and six  
358 right lower m1.

359 **Description and discussion:** 204 isolated teeth show the typical traits of the  
360 genus *Ellobius* (Miller, 1896; Hinton, 1962, Kretzoi, 1969; Coşkun, 2016;  
361 Kryštufek & Shenbrot, 2016; Kryštufek and Vohralík, 2009; Rusin, 2017;  
362 Shenbrot et al., 2016; Tesakov, 2016). *Ellobius* molars are notably  
363 characterized by the presence of roots that are well visible in adults and old  
364 individuals, but not always apparent in young specimens (Coşkun, 2016).  
365 Moreover, *Ellobius* molars lack cement in the re-entrant angles. The *Ellobius*  
366 m1 is composed of the anterior cap (AC), five triangles (T) with three buccal and  
367 four lingual salient angles, and one posterior lobe (PL). Both M3 and m3 are  
368 reduced and smaller than the other molars, with three triangles on the labial  
369 side and two triangles on the lingual side. M1 has three inner and outer folds,  
370 and M2 and M3 have two inner and two outer re-entrant folds. The first and  
371 second upper molars have three triangles on the lingual and labial sides.  
372 However, the re-entrant angle between the first and the second triangles on the  
373 lingual side is more superficial (Gharkheloo and Kivanç, 2003).

374 In Iran, the genus *Ellobius* is currently represented by three species: *Ellobius*  
375 *fuscocapillus*, *Ellobius lutescens* and *Ellobius talpinus* (Firouz, 2005; Kryštufek  
376 & Shenbrot, 2016; Kryštufek and Vohralík, 2009; Moradi Gharkheloo, 2003;  
377 Rusin, 2017; Shenbrot et al., 2016). The m1 is quite similar among these  
378 species, but there are some differences that can help us to differentiate them.

379 The AC is broad in *Ellobius lutescens*, narrow in *Ellobius talpinus* and elongated  
380 in *Ellobius fuscocapillus* (Maul et al., 2015b). The distance between T4 and T5  
381 (W) and the total length (L) differ among the species (Table 5). We have  
382 observed in modern specimens from the Natural History Museum of London  
383 that *Ellobius fuscocapillus* is the largest and *Ellobius talpinus* the smallest.

384 In our sample we identify as *Ellobius* spp. those m1s that are too broken or  
385 digested to distinguish, as well as all the m2, m3, M1, M2 and M3 because of  
386 the lack of discriminant characters. The identification of *Ellobius lutescens* and  
387 *Ellobius fuscocapillus* in the Kaldar material is based on the morphology of the  
388 AC and the measurements (L and W). We do not identify *Ellobius talpinus* in our  
389 sample, as no specimen displays morphological features characteristic of this  
390 species, such as the narrow AC, and because the measured specimens are  
391 larger than *E. talpinus*.

392 **Habitat and distribution:** *Ellobius* species frequent steppes, grasslands and  
393 semi-deserts in eastern Europe and central Asia; these fossorial species are  
394 specialised in subterranean life (Coşkun, 2016; Kryštufek and Vohralík, 2009).  
395 *Ellobius lutescens* is a Palaearctic species distributed across Iran, Iraq,  
396 Azerbaijan, Armenia, Transcaucasia and East Anatolia (Thomas, 1905;  
397 Ellerman and Morrison-Scott, 1951; Darlington, 1957; Osborn, 1962; Walker,

398 1964; Lay, 1967; Hassinger, 1973; Roberts, 1977; Corbet, 1978; Corbet and  
399 Hill, 1991; Wilson and Reeder, 2005; Coşkun, 1997, 2016; Nowak, 1999;  
400 Kryštufek & Shenbrot, 2016). In Iran, this species is found in mountain  
401 grasslands, sandy semi-deserts and steppe areas (Kryštufek & Shenbrot, 2016;  
402 Tesakov, 2016). *Ellobius fuscocapillus* shows a wide range across eastern Iran,  
403 Turkmenistan, Afghanistan and Pakistan. In Iran it is found in open steppes with  
404 loose soil (Shenbrot, Kryštufek & Molur, 2016).

405

406 **Subfamily Cricetinae Fischer, 1817**

407

408 **Genus *Cricetulus* Milne-Edwards, 1867**

409

410 ***Cricetulus migratorius* Pallas, 1773**

411

412 **Material:** 19 isolated teeth. **Layer 1-3:** one isolated tooth; one right lower m3.  
413 **Layer 4:** 13 isolated teeth; three left lower m1, two left upper M2; three right  
414 lower m1, three right upper M1 and two right upper M2. **Layer 5:** five isolated  
415 teeth; three left lower m1 and two right lower m1.

416

417 **Description and discussion:** the first molars (m1 and M1) are brachyodont  
418 and cuspidate, with two longitudinal series of cusps. Each series of cusps  
419 consists of three pairs. The m1 and M1 are the largest and the m3/M3 the  
420 smallest. The lower m3 only has two pairs of cusps (Kryštufek and Vohralík,  
421 2009). We identify *Cricetulus migratorius* in all the layers of Kaldar Cave in  
422 accordance with the measurements and identification keys for molars based on  
423 the morphology and arrangement of the tubercles and cusps provided by  
424 Kryštufek and Vohralík (2009). We also draw comparisons with the reference  
425 collection from Iran, Afghanistan and Azerbaijan housed in the Natural History  
426 Museum of London. The grey hamster, or migratory hamster, is the smallest  
427 hamster species (Bogicevic et al., 2011; Sándor, 2018).

428

429 **Habitat and distribution:** *Cricetulus migratorius* extends from eastern  
430 Europe through Russia and central Asia to Mongolia and western China  
431 (Kryštufek et al., 2017; Kryštufek and Vohralík, 2009). In Iran, this species is  
432 found all over the country. The habitats of this species are mostly dry  
433 grasslands, steppes and semi-deserts. Arid areas with relatively sparse  
434 vegetation are preferred (Kryštufek et al., 2017; Maul et al., 2015a).

435

436 **Genus *Mesocricetus* Nehring, 1898**

437

438 ***Mesocricetus brandti* Nehring, 1898**

439

440 **Material:** 10 isolated teeth. **Layer 4:** three isolated teeth; one left upper M1,  
441 one right lower m1 and one right upper M1. **Layer 5:** seven isolated teeth; four  
442 left upper M1, one right upper M2 and two right upper M1.

443

444 **Description and discussion:** the specimens from Kaldar Cave are  
445 attributed to *Mesocricetus brandti* on the basis of the size and morphology of  
446 the teeth. The molars present a similar morphological pattern to *Cricetulus*  
447 *migratorius*, but are significantly larger in size. The first molars have six

442 tubercles, the second and third molars only four. The largest molars are m1 and  
443 M1, whereas m2/M2 and m3/M3 are reduced (Kryštufek and Vohralík, 2009). In  
444 Iran we also find *Mesocricetus raddei*, which presents a similar morphology of  
445 the teeth to *Mesocricetus brandti*, but compared with the NHM reference  
446 collection of the latter, *Mesocricetus raddei* is bigger

447 **Habitat and distribution:** *Mesocricetus brandti* has the largest distributional  
448 area of the species belonging to the genus *Mesocricetus*, ranging from Anatolia,  
449 Transcaucasia (Armenia, Georgia and Azerbaijan) and southeast Dagestan to  
450 northwest Iran (Qazvin in the east, Lorestan in the south; Lay, 1967). This  
451 species is found at altitudes from sea level up to 2,600 m. However, the primary  
452 range is from 1,000-2,200 m. *Mesocricetus brandti* is found in arid and semi-  
453 arid steppe habitats in lowlands and in mountainous areas (Kryštufek et al.,  
454 2015; Kryštufek and Vohralík, 2009; Neumann et al., 2017).

455

456

**Family Muridae Illiger, 1811**

457

**Subfamily Gerbillinae Gray, 1825**

458

**Genus *Meriones*, Illiger 1811**

459

***Meriones cf. persicus* Blanford, 1875**

460

461

462

463

464

465

**Material:** 157 isolated teeth. **Layer 1-3:** three isolated teeth; two left upper  
M1 and one right lower m1. **Layer 4:** 65 isolated teeth; 21 m2; four m3; 17 left  
lower m1; eight right upper M1, five left upper M1; 10 right lower m1. **Layer 5:**  
88 isolated teeth; eight m3; 21 m2; 18 left lower m1, 10 left upper M1, 16 right  
upper M1 and 15 right lower m1.

466

467

468

469

470

471

472

**Description and discussion:** the genus *Meriones* is one of the most diverse  
among the tribe Gerbillini in the Palaearctic region, particularly in arid regions of  
Asia (Darvish et al., 2011; Denys, 2017). The *Meriones* species reported in Iran  
are: *Meriones crassus*, *Meriones hurrianae*, *Meriones lybicus*, *Meriones*  
*meridianus*, *Meriones persicus*, *Meriones tristrami*, *Meriones vinogradovi* and  
*Meriones zarudnyi* (Darvish, 2011; Dianat et al., 2017; Kryštufek and Vohralík,  
2009; Souttou and Denys, 2012).

473

474

475

476

477

478

479

480

481

The material from Kaldar Cave attributed to the genus *Meriones* displays the  
typical morphology of this group, including semi-hypsodont molars with  
prismatic enamel triangles linked by a longitudinal crest and with no trace of  
cusps. In our sample, we identify first upper molars (M1) with three roots, which  
is characteristic of *Meriones persicus* and *Meriones tristrami*. Unfortunately, the  
dental morphology of *Meriones persicus* and *Meriones tristrami* is very similar;  
there are three roots in m1, the second molars have two transverse plates and  
two roots, whereas the third molars are simple and rounded with a single root  
(Coşkun, 2016; Kryštufek and Vohralík, 2009).

482

483

484

485

Given its current distribution and the morphological traits observed in the  
reference collection from Iran, Azerbaijan and Pakistan housed in the Natural  
History Museum of London, we provisionally attribute our specimens to  
*Meriones cf. persicus*, especially in the light of the number of roots and the

486 morphology of M1 and m1, pending a revision of the Middle Eastern species of  
487 the genus.

488 **Habitat and distribution:** the genus *Meriones* is distributed across North  
489 Africa, Central Asia, Transcaucasia, Turkey and Pakistan (Darvish et al., 2014;  
490 Stoetzel et al., 2017). It lives mostly in dry steppes of short or tall grass, on  
491 open hillside, among rocky outcrops in desolate steppes, or in open dry  
492 meadows. The distribution of *Meriones persicus* ranges from the Caucasus  
493 (including the southeastern foothills of the Lesser Caucasus and the Talysh  
494 Plateau in Azerbaijan) in the west, through northeastern Iraq and Iran to  
495 Turkmenistan, Afghanistan (Habibi, 2004) and Pakistan, where it is widely  
496 distributed. It generally occurs in arid, rocky or mountainous regions (Kryštufek  
497 and Vohralík, 2009; Molur & Sozen, 2016).

498

499

**Family Dipodidae Fischer, 1817**

500

**Genus *Allactaga* Cuvier, 1837**

501

***Allactaga* sp.**

502

503 **Material:** two isolated teeth. **Layer 4:** one indet. **Layer 5:** one right lower m3.

504 **Description and discussion:** this rodent group is poorly known in the  
505 Middle East (Shenbrot, 2009) and sometimes there is a size overlap between  
506 the species. In our sample, we only found two items attributed to *Allactaga* sp.  
507 on the basis of the complete lower m3, which presents a morphology with two  
508 inner folds and one outer fold; the other tooth is broken, which prevents any  
509 precise identification.

510 **Habitat and distribution:** in Iran four species are currently present:  
511 *Allactaga elater*, *Allactaga euphratica*, *Allactaga firouzi* and *Allactaga hotsoni*  
512 (Karami et al., 2008). The different species are morphologically very close and  
513 remain poorly studied. They are mainly found in steppe vegetation and semi-  
514 desert areas (Shenbrot, 2009).

515

516

**Family Gliridae Thomas, 1897**

517

**Genus *Myomimus* Ognev, 1924**

518

***Myomimus* sp.**

519

520 **Material:** five isolated teeth, **Layer 5:** five isolated teeth, one right lower m1,  
521 three right lower m2 and one left lower m2.

522 **Description and discussion:** the genus *Myomimus* is present in Iran with  
523 two species, *Myomimus personatus* and *Myomimus setzeri* (Firouz, 2005;  
524 Gerrie & Kennerley, 2017; Karami et al., 2008; Kennerley & Kryštufek, 2019).  
525 Regarding the remains found at Kaldar, the m1 is of a trapezium-like shape,  
526 and its anterior part tends to be narrower than the posterior part. The m1 has  
527 three roots, two in the anterior part and one in the posterior part. The m2 is  
528 subrectangular, and its occlusal pattern is simpler than in the m1. There are  
529 three roots in total, two in the anterior part and one in the posterior part (Kaya

530 and Kaymakçı, 2018; Kryštufek and Vohralík, 2009). The two species are  
531 similar to one another and poorly studied. Consequently, we were unable to  
532 identify the Kaldar material precisely. Moreover, the reference collection of the  
533 Natural History Museum of London only houses *Myomimus personatus*  
534 specimens, which could therefore not be compared with *Myomimus setzeri*.

535 **Habitat and distribution:** these species are not well known as regards their  
536 distribution. They are mainly found in desert areas (Gerrie & Kennerley, 2017;  
537 Kennerley & Kryštufek, 2019).

538

539

**Family Muridae Illiger , 1811**  
**Genus Apodemus Kaup, 1829**  
**Apodemus sp.**

541

542

543 **Material:** 13 isolated teeth. **Layer 1-3:** two isolated teeth; one left lower m1  
544 and one left lower m2; **Layer 4:** six isolated teeth; three left lower m1, two right  
545 lower m1 and one left upper M1. **Layer 5:** five isolated teeth; two left lower m1,  
546 one right lower m1, one right upper M1 and one m2.

547 **Description and discussion:** the first lower molar (m1) can be seen to  
548 present a low occlusal surface with six main cusps. The anterolabial and  
549 posterolabial cusps of m1 converge in an X-shape. The posterior cusp of m1 is  
550 low, rounded and well developed, with two or three secondary cusps in the  
551 labial part, and a mesial tubercle. We attribute the remains found in Kaldar  
552 Cave to *Apodemus* sp. because they present the traits characteristic of the  
553 genus *Apodemus* (Amori et al., 2016; Bogicevic et al., 2011; Knitlová and  
554 Horáček, 2017; Kryštufek and Vohralík, 2009; López-García, 2008).

555 **Habitat and distribution:** five *Apodemus* species are currently recognized  
556 in Iran: *A. hyrcanicus*, *A. flavicollis*, *A. witherbyi*, *A. avicennicus* and *A.*  
557 *uralensis*, all belonging to the *Sylvaemus* sub-genus (Jangjoo et al., 2011).  
558 *Apodemus* has a large distribution range extending from Great Britain across  
559 much of continental Europe to the Urals. It also extends east through Turkey to  
560 western Armenia, the Zagros Mountains of Iran and south to Syria, Lebanon  
561 and Israel. It inhabits a variety of woodland habitats (Amori et al., 2016).

562

563

**Genus Mus Linnaeus, 1758**  
**Mus cf. musculus Linnaeus, 1758**

564

565

566 **Material:** three isolated teeth. **Layer 4:** one isolated tooth; one left upper M1.  
567 **Layer 5:** two isolated teeth; one indeterminate and one left lower m1.

568 **Description and discussion:** as in other murines, the first upper molar (M1)  
569 has three rows of tubercles: the first (t1, t2, t3) and second (t4, t5 and t6) groups  
570 situated in the anterior part have three tubercles, and the third group (t7 and t9)  
571 has two tubercles (Darviche et al., 2006). In Iran (Kryštufek and Vohralík, 2009)  
572 both *Mus musculus domesticus* and *Mus macedonicus* may be found.

573 The specimens from Kaldar Cave fit well with *M. musculus* as regards the upper  
574 M1 morphology: the lingual row of cusps (t1 and t4) is shifted posteriorly; cusp  
575 t7 is reduced to an enamel ridge; distal cusps t8 and t9 leave no space for a  
576 posterior cingulum or posterolabial cusp t12 (Siahsarvie and Darvish, 2008).  
577 The dental ends of the mesial and central cusps on m1 fuse early; the  
578 mesiolabial cusp is small. Upper molars normally have three roots each, one  
579 lingual and two labial, whereas lower molars are two-rooted (one anterior and  
580 one posterior) (Kryštufek and Vohralík, 2009). Despite these observations,  
581 bearing in mind the high intra-specific morphological variability, the low quantity  
582 of material and the bad state of preservation of some teeth (Fig. 2.13), we only  
583 attribute the Kaldar material to *M. cf. musculus*.

584 **Habitat and distribution:** *Mus musculus* is a commensal species, well  
585 distributed throughout the world: it is present over all the continents except  
586 Antarctica. It is found in a wide range of habitats but tends not to be found in  
587 forest and deserts. *Mus musculus* is ecologically highly opportunistic but a weak  
588 competitor; it can cope with aridity and can also expand into the desert  
589 (Kryštufek and Vohralík, 2009). It is also found in arid habitats along the border  
590 with Syria and Iraq, in desert landscapes and near the Euphrates River  
591 (Kryštufek & Vohralík, 2009; Denys, 2017).

592

#### 593 **4.2. Past landscape and climate at Kaldar Cave**

594

595 The small-mammal assemblages from Layers 4 and 5 of Kaldar Cave are  
596 dominated by the genus *Microtus* (60 individuals in Layer 4 and 79 in Layer 5),  
597 followed by *Ellobius* in Layer 4 (17 individuals) and *Meriones cf. persicus* (17  
598 individuals in Layer 4 and 18 in Layer 5). These species indicate that the  
599 environment in the area was mainly composed of open dry and steppe areas,  
600 although we also found *Apodemus* sp. and *Mus cf. musculus*, which are related  
601 rather to a dense vegetation cover (including trees/bush). All the species  
602 identified at Kaldar Cave still occur in the area today.

603 Layers 1-3 do not yield enough material to draw palaeoclimatic inferences  
604 (MNI < 30). For Layers 4 and 5, the *bioclimatic model* shows similar results  
605 (Table 6). It should be pointed out that some species are not included in the *BM*  
606 data matrix, such as *Myomimus* (present in Layer 4) and *Microtus guentheri*  
607 (Layer 5), because their values did not appear in the *BM* and could not be used  
608 in the analysis. The *BM* based on the small mammals from Kaldar Cave  
609 suggests lower temperatures and lower precipitation than at present in both  
610 Layers 4 and 5 (Table 6). The MAT is around 6°C lower, and there is a higher  
611 temperature amplitude between maximum and minimum mean temperatures.  
612 This indicates that Layers 4 and 5 of Kaldar Cave were deposited during a  
613 colder period, which is not in agreement with the preliminary interpretations of  
614 Bazgir et al. (2017) suggesting a temperate “interstadial”.

615 The climate in Khorramabad nowadays is warm an temperate. The average  
616 mean annual temperature is 16.90°C, the maximum mean temperature occurs

617 in July with 29.60°C and the minimum mean temperature is in January with 5°C  
618 (<https://en.climate-data.org/asia/iran/lorestan/khorramabad-764550/>). This  
619 contrast with the climatic conditions inferred from the *BM* on Kaldar Cave with  
620 lower temperatures and drier conditions.

621 Applying the *habitat weighting method*, our data show a palaeoenvironment  
622 mainly composed of steppes in both levels. In Layer 4, grasslands are also well  
623 represented, notably through the presence of *Microtus guentheri*. In Layer 5,  
624 deserts are the second most represented habitat, thanks to the considerable  
625 presence of *Myomimus* sp. The proportion of rocky areas is also significant,  
626 indicated by the presence of *Chionomys nivalis* and *Meriones* cf. *persicus*  
627 (Figure 3).

628 There thus seems to be no major palaeoenvironmental or palaeoclimatic  
629 change that can explain the cultural shift between Layer 5 (Middle Palaeolithic)  
630 and 4 (Upper Palaeolithic). However, Layer 5 appears slightly colder and drier  
631 than Layer 4, with a higher proportion of desert habitats.

632 We can compare these results with previous studies carried out in Kaldar  
633 Cave using other palaeoenvironmental proxies. Charcoal analyses (Allué et al.,  
634 2018; Bazgir et al., 2017) indicate that there were active water sources or flows,  
635 with specific plant communities characteristic of open forest growing in cool and  
636 dry conditions (Allué et al., 2018). The presence of forested areas is also  
637 supported by the large mammals, with the presence of *Sus scrofa*, *Capreolus*  
638 sp. and *Cervus elaphus* (Bazgir et al., 2017). Several amphibian and squamate  
639 species have also been found (Bazgir et al., 2017): a toad (*Bufo* sp.), an agamid  
640 lizard (Agamidae indet.), a gecko (Gekkonidae indet.), a skink (Scincidae  
641 indet.), a lacertid (Lacertidae indet.), a glass lizard (*Pseudopus* sp.), a sand boa  
642 (*Eryx* sp.), possibly six types of colubrine snakes (Colubrinae indet.), a cobra  
643 (Elapidae indet.), and a viper (Viperidae indet.). Most of these taxa (Agamidae,  
644 *Eryx* and Elapidae) live in savannahs, steppes and deserts, with a way of life  
645 always linked with warm arid areas in rocky or sandy environments. *Pseudopus*  
646 lives in dry and bushy environments, sometimes in open woodlands, but avoids  
647 dense forest areas (Bazgir et al., 2017).

648 Our results based on small mammals, combined with previous studies of  
649 other proxies, thus suggest a mosaic landscape alternating between dry-steppe  
650 areas and wooded patches. Nowadays, the vegetation in the Zagros is a  
651 montane grassland-woodland characterised by steppe of grassland and herbs  
652 with occasional to fairly common trees. The principal local trees are deciduous  
653 oaks and junipers, with maples, walnut, almond and ash at middle elevations,  
654 and *Pistacia* and *Olea* in drier areas (Fiacconi and Hunt, 2015). Thus, the  
655 landscape during the Middle and Upper Pleistocene at Kaldar Cave was similar  
656 to that today, despite a colder climate.

657

#### 658 **4.3. Kaldar Cave in the Middle Eastern context**

659



660 Kaldar Cave is situated in the Khorramabad Valley, which played a  
661 significant role in human adaptation and dispersal during the Quaternary. Some  
662 other caves close to Kaldar, such as Gilvaran, Ghamari and Gar Arjene rock  
663 shelter, have yielded Mousterian and Aurignacian occupations (Bazgir et al.,  
664 2014). Moreover, surveys in Kermanshah have also documented Middle and  
665 Upper Palaeolithic sites (Heydari-Guran and Ghasidian, 2020). None of them  
666 has given rise to small-mammal studies. However, Gilvaran Cave has been  
667 studied from a palaeoenvironmental point of view through charcoal analyses  
668 (Allué et al., 2018), showing a similar pattern to Kaldar, where *Prunus* is also  
669 present and indicates the presence of open forest areas. Similarly, other proxies  
670 such as pollens and charcoals have been analysed at Shanidar (Campana and  
671 Crabtree, 2019; Fiacconi and Hunt, 2015) and Gilvaran (Allué et al., 2018),  
672 indicating similar environmental conditions to Kaldar.

673 Other studies based on small mammals from the Middle East have been  
674 performed in Qesem Cave (Maul et al., 2015a; Smith et al., 2015), Hummal  
675 (Maul et al., 2015b), Azokh Cave (Fernández-Jalvo, 2016), Aghitu-3 Cave  
676 (Frahm, 2019; Kandel et al., 2017; Nishiaki and Akazawa, 2018), Neshar Ramla  
677 (Weissbrod and Zaidner, 2014), Amud Cave (Belmaker and Hovers, 2011),  
678 Dzudzuana Cave (Belmaker et al., 2016) and Karain Cave (Demirel et al.,  
679 2011). These studies did not use *HW* or the *BM* for their palaeoclimatic and  
680 palaeoenvironmental reconstructions, and the sites are not always  
681 contemporary with Kaldar, except Amud Cave (Belmaker and Hovers, 2011),  
682 Aghitu-3 (Djamali et al., 2008; Kandel et al., 2017) and Dzudzuana Cave  
683 (Belmaker et al., 2016) (Table 7).

684 Most of these studies highlight problems in identifying Middle Eastern rodent  
685 species, as faced in the present work. There are some studies of present-day  
686 taxonomy and systematics in Iran, Turkey, Israel, Jordan, Lebanon and Syria  
687 (Abi-said et al., 2014; Darvish et al., 2000; Haddadian Shad et al., 2014; Kopij  
688 and Liven-schulman, 2013; Obuch and Khaleghizadeh, 2012; Shehab et al.,  
689 2013), but these are mostly based on skull morphology and thus not applicable  
690 in archaeological or palaeontological contexts where the remains are broken.  
691 Very few studies provide descriptions of molars with comparative elements,  
692 allowing for the correct identification of fossil specimens. In this context,  
693 comparison with modern specimens from museum collections of genetically  
694 typed specimens is crucial to establish a correct taxonomic reference.

695 Palaeoenvironmental inferences have been drawn on the basis of small-  
696 mammal studies, as well as palynological and anthracological analyses. During  
697 the Upper Pleistocene, small-mammal compositions differ from one site to  
698 another (Belmaker et al., 2016; Kandel et al., 2017) (Table 8), probably because  
699 the sites are not exactly contemporaneous and are likely to belong to different  
700 eco-regions. It is noteworthy that the genera *Microtus*, *Chionomys*, *Cricetulus*,  
701 *Mesocricetus*, *Ellobius* and *Allactaga* are represented in all the sites, allowing  
702 us to reconstruct the species communities of this region. Kaldar is the most  
703 diverse site in terms of small-mammal species.

704 We applied the *habitat weighting method* at other Middle Eastern sites where  
705 small-mammal studies have been performed, namely Aghitu-3 and Dzudzuana  
706 Cave, but these are located in other eco-regions (Figure 1a). Aghitu-3 is located  
707 in Armenia, at an elevation of 1601 m a.s.l. and the current climate is  
708 continental with considerable seasonality in temperature. Dzudzuana Cave is  
709 located in Georgia, at an elevation of 560 m a.s.l., and the current climate is  
710 warm and temperate. The estimations obtained with the *habitat weighting*  
711 *method* (Figure 4) show similar environmental conditions between Kaldar Cave  
712 and Aghitu-3, where the landscape is dominated by steppe (indicated by the  
713 presence of *Ellobius lutescens*, *Mesocricetus brandti*, *Cricetulus migratorius*  
714 and *Allactaga*), with a relatively high percentage of grassland and forests.

715 To ascertain the palaeoclimatic conditions, we calculated and directly  
716 compared our results with Aghitu-3 and Dzudzuana Cave using the *bioclimatic*  
717 *method* (Table 9). The results obtained for Aghitu-3 show higher temperatures  
718 and precipitation than at present, whereas Dzudzuana Cave shows the same  
719 pattern as Kaldar Cave, with drier conditions and lower temperatures than  
720 today. For Amud Cave, it was not possible to calculate *HW* and *BM*, but data  
721 from the literature (Belmaker and Hovers, 2011) indicate a grassland  
722 environment similar to the one that we reconstructed at Dzudzuana Cave.

723

## 724 **5. Conclusions**

725

726 This work represents the first study of a Late Pleistocene rodent assemblage  
727 from the Middle East with palaeoenvironmental and palaeoclimatic  
728 reconstructions, using and adapting the *habitat weighting method* and the  
729 *bioclimatic model* to this area. We identified 1112 rodent remains,  
730 corresponding to a minimum number of 264 individuals. The rodent assemblage  
731 is composed of 13 taxa: six arvicoline (*Microtus socialis*, *Microtus irani*, *Microtus*  
732 *guentheri*, *Chionomys nivalis*, *Ellobius fuscocapillus* and *Ellobius lutescens*),  
733 two cricetine (*Cricetulus migratorius* and *Mesocricetus brandti*), one glirid  
734 (*Myomimus* sp.), one gerbilline (*Meriones* cf. *persicus*), one dipodid (*Allactaga*  
735 sp.) and two murine species (*Apodemus* sp. and *Mus* cf. *musculus*).  
736 Augmenting the preliminary analysis of the material (Bazgir et al., 2017), new  
737 species were identified, such as *Microtus socialis*, *Microtus irani*, *Microtus*  
738 *guentheri*, *Ellobius fuscocapillus* and *Meriones* cf. *persicus*. We also  
739 reconsidered the identification of *Ellobius talpinus*, *Calomyscus* sp. and  
740 *Dryomys* cf. *nitedula*, based on modern specimens from museum collections  
741 and measurements; this is why they do not appear in the new faunal list of  
742 Kaldar Cave.

743 Given the scarcity of studies in this biogeographical region, we encountered  
744 some difficulties in the identification of species, which could slightly affect the  
745 palaeoenvironmental and palaeoclimatic interpretations. In order to counter  
746 these potential errors, further studies of small mammals in this region are

747 necessary, as well as research on discriminant characters in molars, using  
748 reference collections including genetically typed specimens.

749 The palaeoecological analysis of the rodents from Kaldar Cave revealed  
750 lower temperatures and lower precipitation than present-day conditions, and an  
751 environment mainly composed of dry steppes with patches of forested areas.  
752 The results obtained are supported by palynological, anthracological and large-  
753 mammal studies. At a broader geographical scale, colder conditions were also  
754 inferred at Dzudzuana Cave. The genera *Microtus*, *Chionomys*, *Cricetulus*,  
755 *Mesocricetus*, *Ellobius* and *Allactaga* are present at all the Middle East sites  
756 (Aghitu-3, Dzudzuana and Amud) during the Upper Pleistocene, that have  
757 yielded small mammals, allowing us to reconstruct the rodent communities of  
758 the area.

759 Considering all the results from Kaldar Cave and other contemporaneous  
760 sites, we can conclude that both Neanderthals and AMH lived in dry steppes  
761 with patches of forested areas, without major environmental changes occurring  
762 between the Middle and the Late Palaeolithic. Climatic shifts during the MIS 4-3  
763 transition were of a magnitude that did not have a major impact on small  
764 mammals in the region, suggesting that climate change may not have had the  
765 hypothesized effect on the Neanderthal extinction in the Levant.

766

767 **Acknowledgments:** I. Rey-Rodríguez is the beneficiary of a PhD scholarship  
768 funded by the Erasmus Mundus Program (IDQP). J.M. López-García was  
769 supported by a Ramón y Cajal contract (RYC-2016-19386) with financial  
770 sponsorship from the Spanish Ministry of Science, Innovation and Universities.  
771 M. Fernández-García is the beneficiary of a PEJ grant (PEJ2018-005222-P)  
772 funded by the Spanish National Youth Guarantee System and the European  
773 Social Fund. This work was developed within the framework of the projects  
774 2017SGR859, 2017SGR840 and 2017SGR1040 (AGAUR, Generalitat de  
775 Catalunya), and 2018PFRURVB291 (Univ. Rovira i Virigli). We thank the head  
776 of the Research Institute of Cultural Heritage and Tourism (RICHT) (Dr. B.  
777 Omrani) and the head of the Iranian Center for Archaeological Research (ICAR)  
778 (Dr. R. Shirazi) for providing us with the necessary support and permissions in  
779 studying the materials. We thank the head of the Lorestan Cultural Heritage,  
780 Handicraft and Tourism Organization (Mr. A. Ghasemi) for all his support. We  
781 also thank the head of International Collaboration and Ties of the RICHT (Mrs.  
782 M. Kholghi) for all her cooperation and help. B. Bazgir received his PhD  
783 scholarship from the Fundación Atapuerca, for which he is grateful. Laxmi  
784 Tumung received her PhD scholarship from the Erasmus Mundus Programme  
785 (IDQP). We would like to thank Roberto Portela Miguez, Senior Curator in  
786 Charge of Mammals, for his help with the reference collection in the Natural  
787 History Museum of London. We would like to thank Rupert Glasgow for  
788 reviewing the English language of the manuscript. We also want to thank to the  
789 Editor Prof. José S. Carrion and the two anonymous reviewers for their

790 comments and suggestions that strongly improve the final version of the  
791 manuscript.

792

## 793 **References**

794

795 Abi-Said, M.R., Shehab, A.H., Amr, Z.S., 2014. Diet of the Barn Owl. Jordan  
796 Journal of Biological Sciences, Vol. 7, N° 2, 109–112.

797 Allué, E., Expósito, I., Tumung, L., Ollé, A., Bazgir, B., 2018. Early evidence of  
798 *Prunus* and *Prunus* cf. *amygdalus* from Palaeolithic sites in the Khorramabad  
799 Valley, western Iran. Comptes Rendus Palevol 17, 335–345.  
800 <https://doi.org/10.1016/j.crpv.2018.01.001>

801 Amori, G. 1999. *Chionomys nivalis*. In: A. J. Mitchell-Jones, G. Amori, W.  
802 Bogdanowicz, B. Kryštufek, P. J. H. Reijnders, F. Spitzenberger, M. Stubbe, J.  
803 B. M. Thissen, V. Vohralík and J. Zima (eds), *The Atlas of European Mammals*,  
804 Academi Press, London, UK

805 Amori, G., Hutterer, R., Kryštufek, B., Yigit, N., Mitsain, G. & Palomo, L.J., 2016.  
806 *Apodemus flavicollis*. The IUCN Red List of Threatened Species 2016:  
807 e.T1892A115058023. 8235.  
808 [https://doi.org/http://dx.doi.org/10.2305/IUCN.UK.2016-](https://doi.org/http://dx.doi.org/10.2305/IUCN.UK.2016-3.RLTS.T1892A22423256.en)  
809 [3.RLTS.T1892A22423256.en](https://doi.org/http://dx.doi.org/10.2305/IUCN.UK.2016-3.RLTS.T1892A22423256.en)

810 Amr, A., 2015. *Microtus guentheri* , *The IUCN Red List of Threatened*  
811 *Species* 2016: e.T13463A22349143.

812 Andrews, P., 1990. Owls, Caves and Fossils, Owls, Caves and Fossils.  
813 <https://doi.org/10.2307/3889096>

814 Andrews, P., 2006. Taphonomic effects of faunal impoverishment and faunal  
815 mixing. Palaeogeography, Palaeoclimatology, Palaeoecology 241, 572–589.  
816 <https://doi.org/10.1016/j.palaeo.2006.04.012>

817 Aşan Baydemir, N., Duman, L., 2009. Molar patterns in *Microtus guentheri*  
818 (Danford and Alston, 1880) (Mammalia: Rodentia) from Kirikkale province.  
819 Journal of Applied Biological Sciences 3, 47–54.

820 Bazgir, B., Ollé, A., Tumung, L., Becerra-Valdivia, L., Douka, K., Higham, T., Van  
821 Der Made, J., Picin, A., Saladié, P., López-García, J.M., Blain, H.-A., Allué, E.,  
822 Fernández-García, M., Rey-Rodríguez, I., Arceredillo, D., Bahrololoumi, F.,  
823 Azimi, M., Otte, M., Carbonell, E., 2017. Understanding the emergence of  
824 modern humans and the disappearance of Neanderthals: Insights from Kaldar  
825 Cave (Khorramabad Valley, Western Iran). Scientific Reports 7.  
826 <https://doi.org/10.1038/srep43460>

827 Bazgir, B., Otte, M., Tumung, L., Ollé, A., Deo, S.G., Joglekar, P., López-García,  
828 J.M., Picin, A., Davoudi, D., van der Made, J., 2014. Test excavations and initial  
829 results at the middle and upper paleolithic sites of Gilvaran, Kaldar, Ghamari  
830 caves and Gar Arjene Rockshelter, Khorramabad Valley, western Iran. Comptes  
831 Rendus - Palevol 13, 511–525. <https://doi.org/10.1016/j.crpv.2014.01.005>

832 Becerra-Valdivia, L., Douka, K., Comeskey, D., Bazgir, B., Conard, N.J., Marean,  
833 C.W., Ollé, A., Otte, M., Tumung, L., Zeidi, M., Higham, T.F.G., 2017.

834 Chronometric investigations of the Middle to Upper Paleolithic transition in the  
835 Zagros Mountains using AMS radiocarbon dating and Bayesian age modelling.  
836 Journal of Human Evolution 109, 57–69.  
837 <https://doi.org/10.1016/j.jhevol.2017.05.011>

838 Belmaker, M., Bar-Yosef, O., Belfer-Cohen, A., Meshveliani, T., Jakeli, N., 2016.  
839 The environment in the Caucasus in the Upper Paleolithic (Late Pleistocene):  
840 Evidence from the small mammals from Dzudzuana cave, Georgia. Quaternary  
841 International 425, 4–15. <https://doi.org/10.1016/j.quaint.2016.06.022>

842 Belmaker, M., Hovers, E., 2011. Ecological change and the extinction of the  
843 Levantine Neanderthals: Implications from a diachronic study of micromammals  
844 from Amud Cave, Israel. Quaternary Science Reviews 30, 3196–3209.  
845 <https://doi.org/10.1016/j.quascirev.2011.08.001>

846 Blain, H.-A., Bailon, S., Cuenca-Bescós, G., 2008. The Early–Middle Pleistocene  
847 palaeoenvironmental change based on the squamate reptile and amphibian  
848 proxies at the Gran Dolina site, Atapuerca, Spain. Palaeogeography,  
849 Palaeoclimatology, Palaeoecology 261, 177–192.  
850 <https://doi.org/10.1016/j.palaeo.2008.01.015>

851 Bogicevic, K., Nenadic, D., Mihailovic, D., Lazarevic, Z., Milivojevic, J., 2011. Late  
852 Pleistocene rodents (Mammalia: Rodentia) from the Baranica cave near  
853 Knjaževac (eastern Serbia): Systematics and palaeoecology. Rivista Italiana di  
854 Paleontologia e Stratigrafia, Vol. 117, N°2, 331-346.

855 Campana, D. V., Crabtree, P., 2019. Evidence for skinning and craft activities  
856 from the Middle Paleolithic of Shanidar Cave, Iraq. Journal of Archaeological  
857 Science: Reports 25, 7–14. <https://doi.org/10.1016/j.jasrep.2019.03.024>

858 Corbet, G.B., 1978. The Mammals of the Palearctic Region: A Taxonomic  
859 Review. London, Brit. Mus.(Nat. Hist.). Cornell Univ. Press. 117- 118.

860 Corbet, G.B. and Hill, J.E., 1991. A World List of Mammalian Species. 3<sup>rd</sup> ed.  
861 London, UK: British Museum (Natural History).

862 Coşkun, Y., 2016. Review of unique odd chromosome-numbered underground  
863 rodent species of the Palearctic region: *Ellobius Lutescens* Thomas 1897  
864 (Rodentia: Cricetidae). Turkish Journal of Zoology 40, 831–841.  
865 <https://doi.org/10.3906/zoo-1509-53>

866 Coşkun, Y., 1999. Morphological characteristics of *Meriones tristrami* Thomas,  
867 1892 (Rodentia: Gerbillinae) from Diyarbakır, Turkey. Turk. J. Zool 23, 345–  
868 355.

869 Coşkun, Y., 1997. *Ellobius lutescens* Thomas, 1897 (Rodentia: Cricetidae) Turk.  
870 J. of Zoology. 21, 349-354.

871 Darlington, P.J., 1957. Zoogeography: The Geographical Distribution of Animals.  
872 New York, NY, USA: John Wiley and Sons.

873 Darviche, D., Orth, A., Michaux, J., 2006. *Mus spretus* et *M. musculus* (Rodentia,  
874 Mammalia) en zone méditerranéenne: Différenciation biométrique et  
875 morphologique: Application à des fossiles marocains pléistocènes. Mammalia  
876 70, 90–97. <https://doi.org/10.1515/MAMM.2006.010>

877 Darvish, J., Mohammadi, Z., Mahmoudi, A., Siahsharvie, R., 2014. Faunistic and

878 taxonomic study of Rodents from northwestern Iran. Iranian Journal of Animal  
879 Biosystematics (IJAB) 10, 119–136.

880 Darvish, J., 2011. Morphological comparison of fourteen species of the genus  
881 *Meriones* Illiger , 1811 ( Rodentia : Gerbillinae ) from Asia and North Africa.  
882 Iranian Journal of Animal Biosystematics 7, 49–74.

883 Darvish, J., Ghiyasi, R., Khosravi, M., 2000. Recognition of rodents of Robat  
884 Sharaf pellets owl by morphological and neontological studies. Journal of  
885 Sciences 12.

886 Denys, C., 2017. Subfamily Deomyinae, Gerbillinae, Leimacomyinae,  
887 Lophiomyinae species accounts. Pp. 598-650. in : Wilson, D.E., Lacher, T.E.,  
888 Jr. & Mittermeier, R.A. eds. Handbook of the Mammals of the World. Vol.7.  
889 Rodents II. Lynx Edicions, Barcelona.

890 Demirel, A., Andrews, P., Yalçinkaya, I., Ersoy, A., 2011. The taphonomy and  
891 palaeoenvironmental implications of the small mammals from Karain Cave,  
892 Turkey. Journal of Archaeological Science 38, 3048–3059.  
893 <https://doi.org/10.1016/j.jas.2011.07.003>

894 Dianat, M., Darvish, J., Cornette, R., Aliabadian, M., Nicolas, V., 2017.  
895 Evolutionary history of the Persian Jird, *Meriones persicus*, based on genetics,  
896 species distribution modelling and morphometric data. Journal of Zoological  
897 Systematics and Evolutionary Research 55, 29–45.  
898 <https://doi.org/10.1111/jzs.12145>

899 Djamali, M., de Beaulieu, J.L., Shah-hosseini, M., Andrieu-Ponel, V., Ponel, P.,  
900 Amini, A., Akhiani, H., Leroy, S.A.G., Stevens, L., Lahijani, H., Brewer, S., 2008.  
901 A late Pleistocene long pollen record from Lake Urmia, NW Iran. Quaternary  
902 Research 69, 413–420. <https://doi.org/10.1016/j.yqres.2008.03.004>

903 Ellerman, J.R, and Morrison-Scott, T.C.S., 1951. Checklist of Palearctic and  
904 Indian Mammals, 1780 to 1946. Brit. Mus. Nat. Hist. London, 1-810.

905 Evans, E.M.N., Van Couvering, J.A.H., Andrews, P., 1981. Palaeoecology of  
906 Miocene sites in western Kenya. J. Hum. Evol. 10, 99-116.

907 Fernández-Jalvo Y., King T., Yepiskoposyan L. & Andrews P. (eds.), 2016a.  
908 Azokh Cave and the Transcaucasian Corridor, Vertebrate Paleobiology and  
909 Paleoanthropology Series, Springer

910 Fernández-Jalvo, Y., Andrews, P., Denys, C., Sesé, C., Stoetzel, E., Marin-  
911 Monfort, D., Pesquero, D., 2016b. Taphonomy for taxonomists: Implications of  
912 predation in small mammal studies. Quaternary Science Reviews 139, 138–  
913 157. <https://doi.org/10.1016/j.quascirev.2016.03.016>

914 Fiacconi, M., Hunt, C.O., 2015. Pollen taphonomy at Shanidar Cave (Kurdish  
915 Iraq): An initial evaluation. Review of Palaeobotany and Palynology 223, 87–93.  
916 <https://doi.org/10.1016/j.revpalbo.2015.09.003>

917 Firouz, E., 2005. The complete fauna of Iran. Ed. I.B.Tauris & Co Ltd

918 Frahm, E., 2019. Upper Palaeolithic Settlement and Mobility in the Armenian  
919 Highlands : Agent-Based Modeling , Obsidian Sourcing , and Lithic Analysis at  
920 Aghitu-3 Cave.

921 Gerrie, R., Kennerley, R., 2017. *Myomimus personatus*. The IUCN Red List of

922 Threatened Species 2017: e.T14088A22222124 8235.  
923 <https://doi.org/http://dx.doi.org/10.2305/IUCN.UK.2017->  
924 [2.RLTS.T14088A22222124.en](https://doi.org/http://dx.doi.org/10.2305/IUCN.UK.2017-2.RLTS.T14088A22222124.en)

925 Gharkheloo, M., Kivanç, E., 2003, A study on the morphology, karyology and  
926 distribution of *Ellobius* Fischer, 1814 (Mammalia: Rodentia) in Iran. Turkish  
927 Journal of Zoology 27(4):281-292

928 Golenishchev, F.,Malikov, V., Nazari, F., Vaziri, A.,Sablina, O., Polyakov, A.,  
929 2002. New species of vole of “*guentheri* “ group (Rodentia, Arvicolinae,  
930 *Microtus*) from Iran. Russia Journal of Theriology 1 (2), 117-123

931 Golenishchev, F., Malikov, V., Petrova, T., Bodrov, S., Abramson, N., 2019.  
932 Toward assembling a taxonomic puzzle: Case study of Iranian gray voles of the  
933 subgenus *Microtus* (Rodentia, Cricetidae). Mammalian Biology 94, 98–105.  
934 <https://doi.org/10.1016/j.mambio.2018.06.007>

935 Habibi, K. 2004. Mammals of Afghanistan. Zoo Outreach Organisation/USFWS,  
936 Coimbatore, India.

937 Haddadian Shad, H., Darvish, J., Mohammadian, T., Mahmoudi, A., Alaie Kakhki,  
938 N., Ghanbarifardi, M., Molavi, F., Barani-Beiranvand, H., 2014. Preliminary  
939 study of rodents using pellets of predatory birds in Iran. Iranian Journal of  
940 Animal Biosystematics 10, 36–50.

941 Hassinger, J.D., 1973. A survey of the mammals of Afghanistan: Resulting from  
942 the 1965 Street Expedition (Excluding Bats). Fieldiana Zoology, Vol. 60.  
943 Chicago, IL, USA: Field Museum of Natural History.

944 Hernández Fernández, M., 2001. Bioclimatic discriminant capacity of terrestrial  
945 mammal faunas. Global Ecology and Biogeography 10, 189–204.  
946 <https://doi.org/10.1046/j.1466-822x.2001.00218.x>

947 Hernandez Fernández, M., Peláez-Campomanes, P., 2003. The bioclimatic  
948 model: A method of palaeoclimatic qualitative inference based on mammal  
949 associations. Global Ecology and Biogeography 12, 507–517.  
950 <https://doi.org/10.1046/j.1466-822X.2003.00057.x>

951 Hernández Fernández, M., Álvarez Sierra, M.Á., Peláez-Campomanes, P., 2007.  
952 Bioclimatic analysis of rodent palaeofaunas reveals severe climatic changes in  
953 Southwestern Europe during the Plio-Pleistocene. Palaeogeography,  
954 Palaeoclimatology, Palaeoecology 251, 500–526.  
955 <https://doi.org/10.1016/j.palaeo.2007.04.015>

956 Heydari-Guran, S., Ghasidian, E., 2020. Late Pleistocene hominin settlement  
957 patterns and population dynamics in the Zagros Mountains: Kermanshah  
958 region. Archaeological Research in Asia 21, 100161.  
959 <https://doi.org/10.1016/j.ara.2019.100161>

960 Hinton, M.A.C., 1926. Monograph of the Voles and Lemmings (Microtinae) Living  
961 and Extinct. London: British Museum (Natural History). Vol.1. 488 p.

962 Jangjoo, M., J.Darvish & J. D. Vign 2011. Application of outline analysis on fossil  
963 and modern specimens of *Apodemus*. – Iranian J. Anim. Biosystem., 7 (2): 143-  
964 155.

965 Kandel, A.W., Gasparyan, B., Allué, E., Bigga, G., Bruch, A.A., Cullen, V.L.,

966 Frahm, E., Ghukasyan, R., Gruwier, B., Jabbour, F., Miller, C.E., Taller, A.,  
967 Vardazaryan, V., Vasilyan, D., Weissbrod, L., 2017. The earliest evidence for  
968 Upper Paleolithic occupation in the Armenian Highlands at Aghitu-3 Cave.  
969 Journal of Human Evolution 110, 37–68.  
970 <https://doi.org/10.1016/j.jhevol.2017.05.010>

971 Karami, M., Hutterer, R., Benda, P., Siahsarvie, R., Kryštufek, B., 2008.  
972 Annotated check-list of the mammals of Iran. Lynx (Praha) 39, 63–102.

973 Kaya, F., Kaymakçı, N., 2018. Systematics and dental microwear of the late  
974 Miocene Gliridae (Rodentia, Mammalia) from Hayranlı, Anatolia: Implications for  
975 paleoecology and paleobiodiversity. Palaeontologia Electronica 16.  
976 <https://doi.org/10.26879/385>

977 Kennerley, R., Kryštufek, B., 2019. *Myomimus setzeri*. The IUCN Red List of  
978 Threatened Species 2019: e.T14089A22222049. 8235.  
979 [https://doi.org/http://dx.doi.org/10.2305/IUCN.UK.2019-](https://doi.org/http://dx.doi.org/10.2305/IUCN.UK.2019-1.RLTS.T14089A22222049.en)  
980 [1.RLTS.T14089A22222049.en](https://doi.org/http://dx.doi.org/10.2305/IUCN.UK.2019-1.RLTS.T14089A22222049.en)

981 Knitlová, M., Horáček, I., 2017. Late Pleistocene-Holocene paleobiogeography of  
982 the genus *Apodemus* in Central Europe. PLoS ONE 12, 1–23.  
983 <https://doi.org/10.1371/journal.pone.0173668>

984 Kopij, G., Liven-Schulman, I., 2013. Zoology in the Middle East Diet of the Lesser  
985 Kestrel, *Falco naumanni*, in Israel 7140.  
986 <https://doi.org/10.1080/09397140.2012.10648914>

987 Kretzoi, M., 1969. Skizze einer Arvicoliden Phylogenie -Stand 1969 // Vertebrata  
988 Hungarica. Vol.11. No.1–2. P.155–193.

989 Kryštufek, B., Bukhnikashvili, A., Sozen, M., Isfendiyaroglu, S., 2017. *Cricetulus*  
990 *migratorius*. The IUCN Red List of Threatened Species 2016:  
991 e.T5528A115073390 8235.  
992 [https://doi.org/http://dx.doi.org/10.2305/IUCN.UK.2016-](https://doi.org/http://dx.doi.org/10.2305/IUCN.UK.2016-3.RLTS.T5528A115073390)  
993 [3.RLTS.T5528A115073390](https://doi.org/http://dx.doi.org/10.2305/IUCN.UK.2016-3.RLTS.T5528A115073390)

994 Kryštufek, B., Yigit, N., Amori, G., 2015. *Mesocricetus brandti*, Brandt ' s  
995 Hamster. The IUCN Red List of Threatened Species 2008: e.T13220A3421550.  
996 8235.  
997 [https://doi.org/http://dx.doi.org/10.2305/IUCN.UK.2008.RLTS.T13220A3421550.](https://doi.org/http://dx.doi.org/10.2305/IUCN.UK.2008.RLTS.T13220A3421550.en)  
998 [en](https://doi.org/http://dx.doi.org/10.2305/IUCN.UK.2008.RLTS.T13220A3421550.en)

999 Kryštufek, B., Shenbrot, G., 2016. *Ellobius lutescens*, Transcaucasian Mole  
1000 Vole. The IUCN Red List of Threatened Species 2016: e.T7655A22340006.  
1001 8235. [https://doi.org/http://dx.doi.org/10.2305/IUCN.UK.2016-](https://doi.org/http://dx.doi.org/10.2305/IUCN.UK.2016-2.RLTS.T7655A22340006.en)  
1002 [2.RLTS.T7655A22340006.en](https://doi.org/http://dx.doi.org/10.2305/IUCN.UK.2016-2.RLTS.T7655A22340006.en)

1003 Kryštufek, B., 2017. *Chionomys nivalis*, European Snow Vole. The IUCN Red  
1004 List of Threatened Species 2016: e.T4659A115069366 8235.  
1005 [https://doi.org/http://dx.doi.org/10.2305/IUCN.UK.2016-](https://doi.org/http://dx.doi.org/10.2305/IUCN.UK.2016-3.RLTS.T4659A115069366)  
1006 [3.RLTS.T4659A115069366](https://doi.org/http://dx.doi.org/10.2305/IUCN.UK.2016-3.RLTS.T4659A115069366)

1007 Kryštufek, B., Kefelioğlu, H., 2001. Redescription and species limits of *Microtus*  
1008 *irani* Thomas, 1921, and description of a new social vole from Turkey  
1009 (Mammalia: Arvicolinao).



- 1010 Kryštufek, B., Vohralík, V., 2009. Mammals of Turkey and Cyprus, Rodentia II:  
1011 Cricetinae, Muridae, Spalacidae, Calomyscidae, Capromyidae, Hystricidae,  
1012 Castoridae. <https://doi.org/10.1644/10-MAMM-R-221.1>
- 1013 Lay, D.M., 1967. A Study of the Mammals of Iran, Resulting from the Street  
1014 Expedition of 1962-63. *Fieldiana Zool.*, 54: 168-171.
- 1015 López-García, J.M., 2011. Los micromamíferos del Pleistoceno superior de la  
1016 Península Ibérica: Evolución de la diversidad taxonómica y cambios  
1017 paleoambientales y paleoclimáticos. Editorial Académica Española
- 1018 López-García, J.M., Blain, H.-A., Cuenca-Bescós, G., Alonso, C., Alonso, S.,  
1019 Vaquero, M., 2011. Small vertebrates (Amphibia, Squamata, Mammalia) from  
1020 the late Pleistocene-Holocene of the Valdavara-1 cave (Galicia, northwestern  
1021 Spain). *Geobios* 44, 253–269. <https://doi.org/10.1016/j.geobios.2010.10.001>
- 1022 Maul, L.C., Bruch, A.A., Smith, K.T., Shenbrot, G., Barkai, R., Gopher, A., 2015a.  
1023 Palaeoecological and biostratigraphical implications of the microvertebrates of  
1024 Qesem Cave in Israel. *Quaternary International*.  
1025 <https://doi.org/10.1016/j.quaint.2015.04.032>
- 1026 Maul, L.C., Smith, K.T., Shenbrot, G., Bruch, A.A., Wegmüller, F., Le Tensorer,  
1027 J.M., 2015b. Microvertebrates from unit G/layer 17 of the archaeological site of  
1028 Hummal (El Kowm, Central Syria): Preliminary results. *Anthropologie (France)*  
1029 119, 676–686. <https://doi.org/10.1016/j.anthro.2015.10.010>
- 1030 Miller, G.S., 1896. Genera and subgenera of voles and lemmings// North  
1031 American Fauna. Vol.12. P.1–85.
- 1032 Molur, S. & Sozen, M., 2016. *Meriones persicus*, Persian Jird. The IUCN Red List  
1033 of Threatened Species 2016: e.T13166A22433231. 8235.  
1034 <https://doi.org/http://dx.doi.org/10.2305/IUCN.UK.2016->  
1035 [2.RLTS.T13166A22433231.en](https://doi.org/http://dx.doi.org/10.2305/IUCN.UK.2016-2.RLTS.T13166A22433231.en)
- 1036 Moradi Gharkheloo, M., 2003. A Study on the Morphology , Karyology and  
1037 Distribution of *Ellobius* Fischer , 1814 ( Mammalia : Rodentia ) in Iran. *Turkish*  
1038 *Journal of Zoology* 27, 281–292.
- 1039 Neumann, K., Yiğit, N., Fritzsche, P., Çolak, E., Feoktistova, N., Surov, A.,  
1040 Michaux, J., 2017. Genetic structure of the Turkish hamster (*Mesocricetus*  
1041 *brandti*). *Mammalian Biology* 86, 84–91.  
1042 <https://doi.org/10.1016/j.mambio.2017.06.004>
- 1043 Nishiaki, Y., Akazawa, T., 2018. The Middle and Upper Paleolithic Archeology of  
1044 the Levant and Beyond. Replacement of Neanderthals by Modern Humans  
1045 Series 35–47. [https://doi.org/10.1007/978-981-10-6826-3\\_3](https://doi.org/10.1007/978-981-10-6826-3_3)
- 1046 Nowak, R.M., 1999. Walker's Mammals of the World. 6th ed. Baltimore, MD,  
1047 USA: The Johns Hopkins University Press.
- 1048 Obuch, J., Khaleghizadeh, A., 2012. Spatial Variation in the Diet of the Barn Owl  
1049 *Tyto alba* in Iran 6, 103–116.
- 1050 Osborn, D.J., 1962. Rodents of subfamily Microtinae from Turkey. *J. Mammalia*,  
1051 43: 515-529.
- 1052 Rey-Rodríguez, I., Stoetzel, E., López-García, J.M., Denys, C., 2019.  
1053 Implications of modern Barn owls pellets analysis for archaeological studies in

1054 the Middle East. *Journal of Archaeological Science* 111, 105029.  
1055 <https://doi.org/10.1016/J.JAS.2019.105029>

1056 Roberts, T.J., 1977. *The Mammals of Pakistan*. London, UK: Ernst Benn Ltd.

1057 Rusin, M., 2017. *Ellobius talpinus*, Northern Mole Vole. The IUCN Red List of  
1058 Threatened Species 2016: e.T7656A115085720. 8235.  
1059 [https://doi.org/http://dx.doi.org/10.2305/IUCN.UK.2016-](https://doi.org/http://dx.doi.org/10.2305/IUCN.UK.2016-3.RLTS.T7656A22339917.en)  
1060 [3.RLTS.T7656A22339917.en](https://doi.org/http://dx.doi.org/10.2305/IUCN.UK.2016-3.RLTS.T7656A22339917.en)

1061 Sándor, A.D., 2018. Rediscovered after half a century: A new record of the grey  
1062 dwarf hamster, *Cricetulus migratorius* (Mammalia: Cricetidae), in Romania.  
1063 *Turkish Journal of Zoology* 42, 495–498. <https://doi.org/10.3906/zoo-1712-15>

1064 Shehab, A., Daoud, A., Kock, D., Amr, Z., 2013. Zoology in the Middle East Small  
1065 mammals recovered from owl pellets from 7140.  
1066 <https://doi.org/10.1080/09397140.2004.10638061>

1067 Shenbrot, G., Kryštufek, B., Molur, S., 2016. *Ellobius fuscocapillus*, Southern  
1068 Mole Vole. The IUCN Red List of Threatened Species 2016:  
1069 e.T7654A22339730. 8235.  
1070 [https://doi.org/http://dx.doi.org/10.2305/IUCN.UK.2016-](https://doi.org/http://dx.doi.org/10.2305/IUCN.UK.2016-2.RLTS.T7654A22339730.en)  
1071 [2.RLTS.T7654A22339730.en](https://doi.org/http://dx.doi.org/10.2305/IUCN.UK.2016-2.RLTS.T7654A22339730.en)

1072 Shenbrot, G., 2009. On the conspecificity of *Allactaga hotsoni* Thomas, 1920 and  
1073 *Allactaga firouzi* Womochel, 1978 (Rodentia: Dipodoidea). *Mammalia* 73, 231–  
1074 237. <https://doi.org/10.1515/MAMM.2009.043>

1075 Shenbrot, G.I. and Krasnov, B.R. 2005. *An Atlas of the Geographic Distribution of*  
1076 *the Arvicoline Rodents of the World* (Rodentia, Muridae: Arvicolinae). Pensoft  
1077 Publishers, Sofia.

1078 Siahsarvie, R., Darvish, J., 2008. Geometric morphometric analysis of Iranian  
1079 wood mice of the genus *Apodemus* (Rodentia, Muridae). *Mammalia* 72, 109–  
1080 115. <https://doi.org/10.1515/MAMM.2008.020>

1081 Smith, K.T., Christian, L., Flemming, F., Barkai, R., Gopher, A., 2016. The  
1082 microvertebrates of Qesem Cave: A comparison of the two concentrations.  
1083 *Quaternary International* 1–13. <https://doi.org/10.1016/j.quaint.2015.04.047>

1084 Souttou, K., Denys, C., 2012. Small Mammal Bone Modifications in Black-  
1085 Shouldered Kite *Elanus caeruleus* Pellets from Algeria: Implications for  
1086 Archaeological Sites. *Journal of Taphonomy* 10, 1–19.

1087 Stoetzel, E., Cornette, R., Lalis, A., Nicolas, V., Cucchi, T., Denys, C., 2017.  
1088 Systematics and evolution of the *Meriones shawii/grandis* complex (Rodentia,  
1089 Gerbillinae) during the Late Quaternary in northwestern Africa: Exploring the  
1090 role of environmental and anthropogenic changes. *Quaternary Science Reviews*  
1091 164, 199–216. <https://doi.org/10.1016/j.quascirev.2017.04.002>

1092 Tesakov, A.S., 2016. Early Middle Pleistocene *Ellobius* (Rodentia, Cricetidae,  
1093 Arvicolinae) from Armenia. *Russian J. Theriol.* 15 (2): 151–158.

1094 Thomas, O., 1905. *Ellobius woosnami*. *Abstr. Proc. Zool. Soc.* 23; *Proc. Zool.*  
1095 *Soc.* 526 London.

1096 Tsytsulina, K., Kryštufek, B., Yigit, N., Bukhnikashvili, A., Shenbrot, G., 2017.  
1097 *Microtus socialis*, Social. The IUCN Red List of Threatened Species 2016:

1098 e.T13458A115114745.  
1099 8235.https://doi.org/http://dx.doi.org/10.2305/IUCN.UK.2016-  
1100 3.RLTS.T13458A22348936.en  
1101 Walker, E.P., 1964. Mammals of the World. Vol. 2. Baltimore, MD,USA: The  
1102 Johns Hopkins Press.  
1103 Weissbrod, L., Zaidner, Y., 2014. Taphonomy and paleoecological implications of  
1104 fossorial microvertebrates at the Middle Paleolithic open-air site of Nesher  
1105 Ramla, Israel. Quaternary International 331, 115–127.  
1106 <https://doi.org/10.1016/j.quaint.2013.05.044>  
1107 Wilson, D.E. and Reeder, D.M., 2005. Mammal Species of the World.  
1108 Washington, DC, USA: Smithsonian Institution Scholarly Press.  
1109

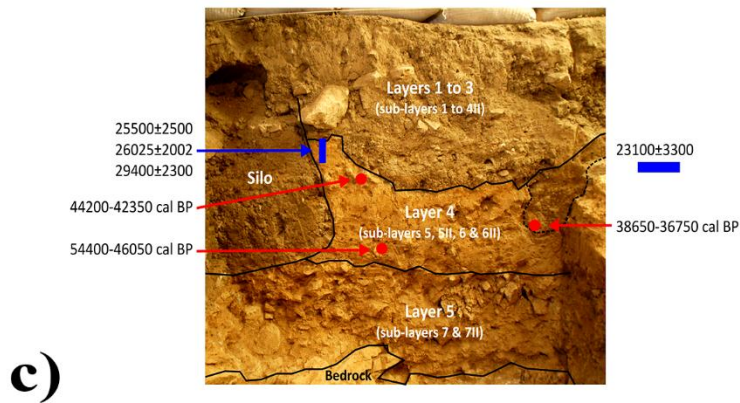
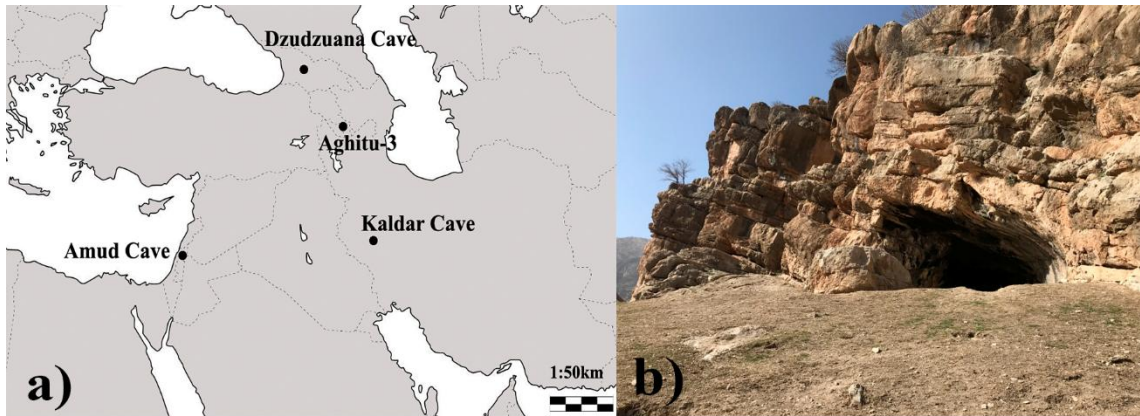


Figure 1: a) Locations of the Late Pleistocene sites with rodent studies in the Middle East, including Kaldar Cave. b) General view of the entrance to Kaldar Cave. c) Stratigraphy of the eastern section of Kaldar Cave, including the location and results of the dated samples, from A. Ollé and B. Bazgir (Bazgir et al., 2017).

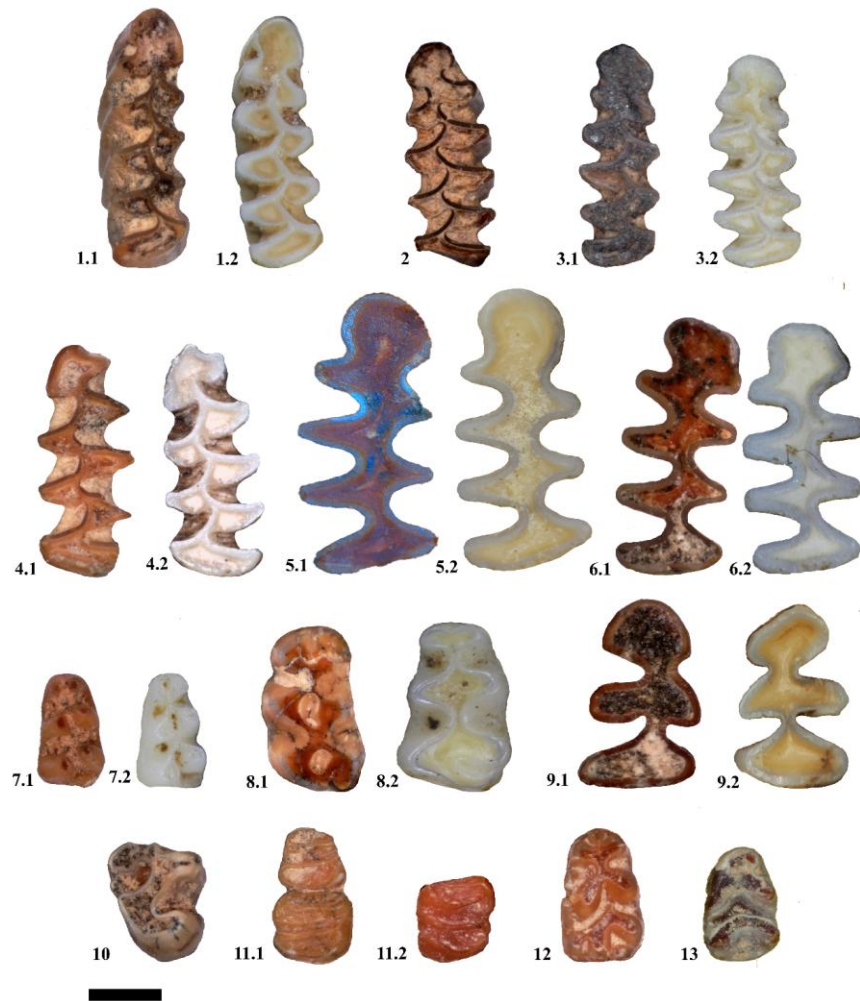


Figure 2: Some rodent species identified at Kaldar Cave in comparison with equivalent (analogue) modern specimens from the NHM of London. **1) *Microtus irani***: 1.1-Kaldar Cave, 2014, Layer 5 (sub-layer 7II), E7, 150-156, right lower m1, number 447. 1.2-modern, NHM205207, Iran (Shiraz), right lower m1; **2) *Microtus guentheri***: 2.1-Kaldar Cave, 2014, Layers 1-3 (sub-layer 4II), F6, 97-107, left lower m1, number 17; **3) *Microtus socialis***: 3.1-Kaldar Cave, 2014, Layer 4 (sub-layer 5II), F7, 115-118, right lower m1, number 106. 3.2-modern, NHM631799, Turkey (Amasya); **4) *Chionomys nivalis***: 4.1-Kaldar Cave, 2014, Layer 4 (sub-layer 5), E6, 94-104, left lower m1, number 542. 4.2-modern, NHM71820, Syria, left lower m1; **5) *Ellobius fuscocapillus***: 5.1-Kaldar Cave, 2014, Layer 4 (sub-layer 5II), E6, 125-130, right lower m1, number 157. 5.2-modern, NHM86101513, Afghanistan, right lower m1; **6) *Ellobius lutescens***: 6.1-Kaldar Cave, 2014, Layer 5 (sub-layer 7II), F6, 130-140, right lower m1, number 319. 6.2-NMH916416, Turkey, right lower m1; **7) *Cricetulus migratorius***: 7.1-Kaldar Cave, 2014, Layer 4 (sub-layer 5II), E6, 135-140, left lower m1, number 259. 7.2-modern, NHM773029, Iran, right lower m1; **8) *Mesocricetus brandti***: 8.1-Kaldar Cave, 2014, Layer 5 (sub-layer 7II), F6, 135-145, left upper M1, number 549. 8.2- modern, NHM193461226, Caucasus, left upper M1; **9) *Meriones cf. persicus***: 9.1-Kaldar Cave, 2014, Layer 5 (sub-layer 7II), F6, 156-166, left lower m1, number 551. 9.2-modern, NHM510434, Iran, left lower m1; **10) *Allactaga* sp.**: 10.1-Kaldar Cave, 2014, Layer 5 (sub-layer 7II), E7, 141-147, right lower m3, number 203; **11) *Myomimus* sp.**: 11.1- Kaldar Cave, 2014, Layer 5 (sub-layer 7II), E7, 141-147, left lower m1 and m2. 11.2-modern, *Myomimus personatus*, NHM67623, Turkey, left lower mandible; **12) *Apodemus* sp.**: 12.1-Kaldar Cave, 2014, Layer 4 (sub-layer 5), E6, 94-104, right m1 and m2, number 547; **13) *Mus cf. musculus***: 13.1-Kaldar Cave, 2014, Layer 5 (sub-layer 7II), 166-174, left lower m1, number 495. Scale 1 mm.

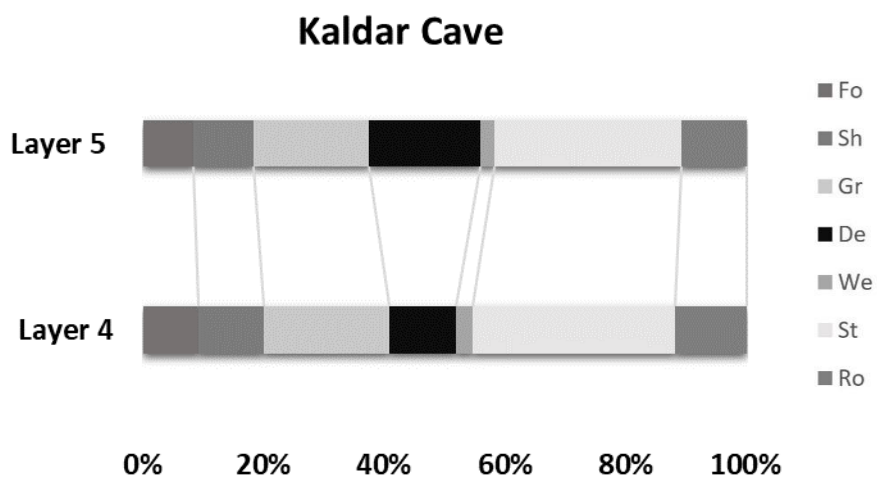


Figure 3: Results of the *habitat weighting method* for Kaldar Cave (Layer 4 and Layer 5). Forest (Fo), Shrubland (Sh), Grassland (Gr), Desert (De), Wetland (We), Steppe (St) and Rocky (Ro).

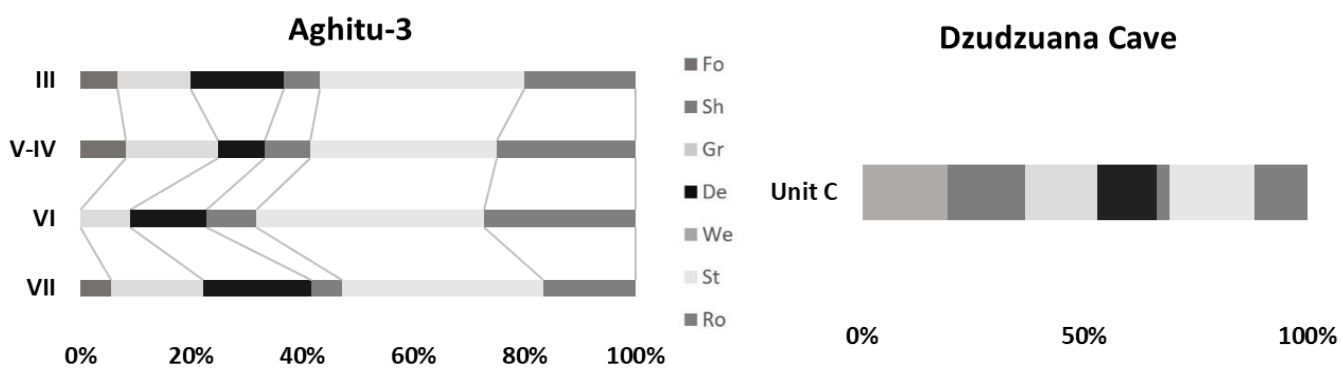


Figure 4: Results of the *habitat weighting method* for Aghitu-3 and Dzudzuana Cave. Forest (Fo), Shrubland (Sh), Grassland (Gr), Desert (De), Wetland (We), Steppe (St) and Rocky (Ro).

Species	Fo	Sh	Gr	De	We	St	Ro
<i>Ellobius lutescens</i>			0.33	0.33		0.33	
<i>Ellobius fuscocapillus</i>						1	
<i>Microtus irani</i>			1				
<i>Microtus guentheri</i>			1				
<i>Microtus socialis</i>		0.5				0.5	
<i>Chionomys nivalis</i>							1
<i>Cricetulus migratorius</i>			0.33	0.33		0.33	
<i>Mesocricetus brandti</i>						1	
<i>Meriones persicus</i>		0.33	0.33				0.33
<i>Allactaga sp.</i>				0.5		0.5	
<i>Apodemus sp.</i>	1						
<i>Mus musculus</i>		0.33	0.33		0.33		
<i>Myomimus sp.</i>				1			

Table 1: scores attributed to each rodent species found at Kaldar Cave according to its ecological requirements, used for the *habitat weighting method*: Forest (Fo), Shrubland (Sh), Grassland (Gr), Desert (De), Wetland (We), Steppe (St) and Rocky (Ro).

Species	I	II	II/III	III	IV	V	VI	VII	VIII	IX
<i>Ellobius lutescens</i>								1		
<i>Ellobius fuscocapillus</i>				0.33	0.33			0.33		
<i>Microtus irani</i>					1					
<i>Microtus socialis</i>					0.5			0.5		
<i>Chionomys nivalis</i>					0.25		0.25		0.25	0.25
<i>Cricetulus migratorius</i>					0.33		0.33	0.33		
<i>Mesocricetus brandti</i>					1					
<i>Meriones persicus</i>				0.5	0.5					
<i>Allactaga sp.</i>				0.5				0.5		
<i>Apodemus sp.</i>							1			
<i>Mus musculus</i>	0.11	0.11	0.11	0.11	0.11	0.11	0.11	0.11	0.11	

Table 2: scores attributed to each rodent species found at Kaldar Cave for the bioclimatic model (in accordance with Hernández-Fernández, 2001; Hernández-Fernández et al., 2007). See text for the significance of the Roman numerals corresponding to the climatic groups.

Taxon	Layer 5			Layer 4			Layers 1-3		
	NISP	MNI	%	NISP	MNI	%	NISP	MNI	%
Indet.	3	-	-	11	-	-	-	-	-
<i>Microtus</i> spp.	292	51	52.33	258	31	48.31	4	3	20
<i>Microtus irani</i>	14	9	2.51	0	0	0.00	1	1	5
<i>Microtus guentheri</i>	0	0	0.00	16	9	3.00	1	1	5
<i>Microtus socialis</i>	35	20	6.27	36	20	6.74	3	3	15
<i>Chionomys nivalis</i>	6	3	1.08	17	12	3.18	2	1	10
<i>Ellobius</i> spp.	80	7	14.34	91	8	17.04	2	2	10
<i>Ellobius fuscocapillus</i>	5	4	0.90	5	3	0.94	1	1	5
<i>Ellobius lutescens</i>	10	6	1.79	10	7	1.87	-	-	-
<i>Cricetulus migratorius</i>	5	3	0.90	14	3	2.62	1	1	5
<i>Mesocricetus brandti</i>	7	4	1.25	3	1	0.56	0	0	0
<i>Meriones</i> cf. <i>persicus</i>	88	18	15.77	65	17	12.17	3	2	15
<i>Allactaga</i> sp.	1	1	0.18	1	1	0.19	0	0	0
<i>Myomimus</i> sp.	5	3	0.90	0	0	0.00	0	0	0
<i>Apodemus</i> sp.	5	2	0.90	6	3	1.12	2	1	10
<i>Mus</i> cf. <i>musculus</i>	2	1	0.36	1	1	0.19	0	0	0
<b>Total</b>	<b>558</b>	<b>132</b>	<b>100.00</b>	<b>534</b>	<b>116</b>	<b>100.00</b>	<b>20</b>	<b>16</b>	<b>100.00</b>

Table 3: Representation of the Kaldar Cave rodent species in terms of number of identified specimens (NISP), minimum number of individuals (MNI) and percentage of the NISP (%).



Species	NS	L (Length)		La (Width T4)		Li (Width T5)		Total Width	
		Mean	Min-Max	Mean	Min-Max	Mean	Min-max	Mean	Max-Min
<b>Reference collection</b>									
<i>Microtus irani</i>	4	3.06	2.98-3.23	0.42	0.40-0.44	0.64	0.62-0.67	1.06	1.03-1.08
<i>Microtus socialis</i>	69	2.78	2.29-3.34	0.42	0.32-0.51	0.6	0.44-0.73	1.02	0.78-1.19
<i>Microtus arvalis</i>	25	2.72	2.45-2.96	0.39	0.32-0.46	0.6	0.50-0.70	1	0.83-1.13
<i>Microtus guentheri</i>	70	2.58	2.2-3						
<b>Kaldar Cave</b>									
<i>Microtus guentheri</i>	17	2.52	2.18-3.01	0.35	0.27-0.43	0.54	0.40-0.68	0.90	0.70-1.10
<i>Microtus irani</i>	15	2.89	2.52-3.39	0.41	0.37-0.50	0.62	0.54-0.70	1.05	0.92-1.18
<i>Microtus socialis</i>	74	2.54	2.06-3.01	0.37	0.28-0.48	0.55	0.40-0.70	0.92	0.70-1.16

Table 4: Measurements of *Microtus* specimens (in mm): NS, number of specimens; L, length; La, T4 width; Li, T5 width.

		<i>Ellobius fuscocapillus</i>				<i>Ellobius lutescens</i>		<i>Ellobius talpinus</i>	
		Layer 5 NISP=5	Layer 4 NISP=5	Layer 1-3 NISP=1	NHM NISP=12	Layer 5 NISP=9	Layer 4 NISP=10	NHM NISP=14	NHM NISP=14
<b>L</b>	<b>Min-Max</b>	3.29-3.84	3.73-3.74	-	3.06-4.05	3.08-3.32	3.05-3.4	3.07-3.3	2.86-3.35
	<b>Mean</b>	3.45	3.74	-	3.53	3.28	3.29	3.21	3.12
<b>W</b>	<b>Min-Max</b>	1.32-1.51	1.40-1.54	-	1.3-1.59	1.20-1.45	1.13-1.48	1.11-1.52	1.09-1.72
	<b>Mean</b>	1.45	1.48	1.5	1.41	1.34	1.32	1.34	1.24

Table 5: Measurements of *Ellobius* specimens (in mm): L, total length; W, width. NHM: Natural History Museum of London. NISP: number of identified specimens.

	Layer 5	SD	Layer 4	SD	Current values
Mean annual temperature	10.90 °C	3.39	11.73°C	3.39	16.90 °C
Maximum mean temperature	23.45 °C	4.77	23.10°C	4.77	29.60 °C
Minimum mean temperature	-1.69 °C	4.66	0.25°C	4.66	5°C
Mean annual precipitation	258.68mm	533.24mm	104.08mm	533.24mm	488mm

Table 6: Bioclimatic model estimates for Kaldar Cave. SD, standard deviation. Current values obtained from: <https://en.climate-data.org/asia/iran/lorestan/khorramabad-764550/>.

Site/Author	Layer	Human culture	Chronology	Environmental conditions	Rodent
Amud Cave (Belmaker and Hovers, 2011)	B4	Neanderthals	68.5 ± 3.4ka	Grassland vegetation	<i>Microtus guentheri</i>
	B2-B1	Neanderthals	56.5 ± 3.5, 57.6 ± 3.7, respectively	Woodland	<i>Apodemus cf. mystacinus</i> and <i>Mus macedonicus</i>
Dzudzuana Cave (Belmaker et al., 2016)	Unit C	Modern human	27-24ka cal BP	Mild and humid	<i>Microtus</i> , <i>Ellobius</i> , <i>Arvicola</i> , <i>Apodemus</i> and <i>Allactaga</i> .
Aghitu-3 (Djamali et al., 2008; Kandel et al., 2017)	Level VII-III	Modern human	The oldest layer is VII with a chronology between 39-36,000 cal BP and the most recent is layer III, between 29-24,000 cal BP	This sequence documents that the climate becomes colder	<i>Microtus</i> spp., <i>Chionomys</i> sp., <i>Arvicola amphibius</i> and <i>Ellobius lutescens</i>

Table 7: Comparison between Middle Eastern sites with small-mammal studies

Taxon	Kaldar Cave			Aghitu-3			Dzudzuana	
	Layers 1-3	Layer 4	Layer 5	VII	VI	V-IV	III	Unit C
<i>Microtus</i> spp.	X	X	X	X	X	X	X	
<i>Microtus</i> cf. <i>arvalis</i>								X
<i>Microtus irani</i>	X		X					
<i>Microtus guentheri</i>	X	X						
<i>Microtus socialis</i>	X	X	X					
<i>Chionomys nivalis</i>	-	X	X	X	X	X	X	X
<i>Clethrionomys glareolus</i>								X
<i>Ellobius</i> spp.	X	X	X					
<i>Ellobius fuscocapillus</i>	X	X	X					
<i>Ellobius lutescens</i>	-	X	X	X				X
<i>Cricetus cricetus</i>								X
<i>Cricetulus migratorius</i>	X	X	X	X		X	X	X
<i>Mesocricetus brandti</i>		X	X	X	X	X	X	X
<i>Meriones</i> cf. <i>persicus</i>	X	X	X					
<i>Allactaga</i> sp.		X	X	X	X		X	X
<i>Myomimus</i> sp.			X					
<i>Apodemus</i> sp.	X	X	X					X
<i>Mus musculus</i>		X	X					X
<i>Arvicola amphibius</i>				X	X	X	X	X

Table 8: comparison of the small-mammal lists from several Upper Palaeolithic sites in the Middle East.

	Aghitu-3						Dzudzuana Cave		
	VII	VI	V-IV	III	SD	Current Values	Unit C	SD	Current Values
Mean annual Temperature	15.46 °C	19.44 °C	19.21 °C	17.87 °C	3.386	8.5 °C	5.09 °C	3.39	9.7 °C
Maximum mean temperature	23.59 °C	24.44 °C	24.09 °C	24 °C	4.772	20.2 °C	18.55 °C	4.77	20.3 °C
Minimum mean temperature	7.31 °C	14.67 °C	14.72 °C	11.96 °C	4.656	-3.8 °C	-8.26 °C	4.66	-1.6 °C
Mean annual precipitation	1169.04 mm	1729.48 mm	1825.99 mm	1484.60 mm	533.236	532 °C	194.98 mm	533.24	868 mm

Table 9: Estimates using the *bioclimatic method* for Aghitu-3 and Dzudzuana Cave. SD, standard deviation. Current values obtained from Kandel et al. (2017) for Aghitu-3 and <https://es.climate-data.org/asia/georgia/imereti/jria-414325/?amp=true> for Dzudzuana Cave.

